University of Évora

ARCHMAT

(ERASMUS MUNDUS MASTER IN ARCHaeological MATerials Science)

Mestrado in Arqueologia e Ambiente (Erasmus Mundus - ARCHMAT)

Application of Laser Technologies in the Restauration of Stained Glass

Xiang Zhang (38424)

Professor Doctor Xermán de la Fuente
Institute of Materials Science of Aragon
Co-supervisor

Professor Doctor Luis Alberto Angurel Lambán
Institute of Materials Science of Aragon
Co-supervisor

Professor Doctor Maria Pilar Alonso Abad
University of Burgos
Co-supervisor

Professor Doctor Nicola Schiavon
University of Évora
Co-supervisor

Évora, Portugal, October 2018

University of Évora

ARCHMAT

(ERASMUS MUNDUS MASTER IN ARCHaeological MATerials Science)

Mestrado in Arqueologia e Ambiente (Erasmus Mundus - ARCHMAT)

Application of Laser Technologies in the Restauration of Stained Glass

Xiang Zhang (38424)

Professor Doctor Xermán de la Fuente
Institute of Materials Science of Aragon
Co-supervisor

Professor Doctor Luis Alberto Angurel Lambán
Institute of Materials Science of Aragon
Co-supervisor

Professor Doctor Maria Pilar Alonso Abad
University of Burgos
Co-supervisor

Professor Doctor Nicola Schiavon
University of Évora
Co-supervisor

Évora, Portugal, October 2018

JURY MEMBERS

President: Cristina Dias
Examiner: Emma Angelini
Supervisor: Nick Schiavon
Partner Member: Federico di Rita

ACKNOWLEDGEMENTS

I wish to thank first of all Professor Xermán de la Fuente and Professor Luis Alberto Angurel Lambán for guiding me through the knowledge and experience in the field of lasers. I would like to thank most especially Professor Luis Alberto Angurel Lambán, who modified my thesis carefully and guided me through the difficulties I faced during the writing process.

I would like to thank Professor Maria Pilar Alonso Abad for the introduction to the background about the history, fabrication, deterioration and restoration of stained glass and for providing the stained glass sample on which this study was performed.

I would also like to express my gratitude to Professor Nicola Schiavon for giving me opportunity to work on this project and also for his trust, patience and understanding.

As well, I would like to mention my colleagues Alejandro Montón Zarazaga，Qiaojun Wu and Wei Shao, who have helped me and supported me in this study.

I would like to express gratitude to the Education, Audiovisual and Culture Executive Agency (EACEA) of the European Commission for rewarding me with a scholarship to attend the Erasmus Mundus Master in Archaeological Materials Science, and to the coordinators and professors participating in ARCHMAT project.

As well, I thank my fellow classmates from ARCHMAT for their friendship and constant support, and for all the fun we have had in the last two years.

Last but not least, I wish to thank my friends and family, without whose encouraging words and unfailing support, I would never have got this far.

CONTENTS

ACKNOWLEDGEMENTS i
LIST OF FIGURES iv
LIST OF TABLES vi
ABSTRACT vii
RESUMO viii
AIMS AND OBJECTIVES ix
CHAPTER 1: LASERS IN STAINED GLASS RESTAURATION 1
1.1.- Stained glass windows 1
1.1.1.- Materials and fabrication techniques 1
1.1.2.- Producing a window from start to finish 7
1.2.- Pathologies and restoration methods 7
1.2.1.- Pathologies 7
1.2.2.- Restoration methods 12
1.3.- Laser cleaning 15
1.3.1.- Laser cleaning in conservation 15
1.3.2.- Principles of laser conservation 16
1.3.3.- Laser cleaning parameters 18
CHAPTER 2: EXPERIMENTAL METHODS 21
2.1.- Laser systems 21
2.1.1.- UV sub-nano laser 21
2.1.2.- n-IR sub-nano laser 21
2.2.- Modes in laser processing 22
2.2.1.- Beam scanning, continuous mode 22
2.2.2.- Burst mode 23
2.2.3.- Bit-map mode 24
2.3.- Characterization techniques 24
2.3.1.- Confocal microscopy 24
2.3.2.- Portable optical microscopy 25

2.3.3.- Scanning electron microscopy 25
2.4.- Materials 26
2.4.1.- Sample of historical stained glass 26
2.4.2.- Samples of commercial modern glass 27
CHAPTER 3: IDENTIFICATION OF ABLATION THRESHOLD IN COMMERCIAL MODERN GLASS 28
3.1.- Effect of using the UV laser to process brown industrial glass 28
3.2.- Effect of using the UV laser to process transparent industrial glass 32
3.3.- Effect of using the n-IR laser to process industrial glass 35
3.4.- Elimination of surface cracks in window glass 36
CHAPTER 4: DEVELOPING LASER PROCESSES TO TREAT LOCALISED AREAS 37
4.1.- Developing a system to define areas where laser treatment has to be performed 37
4.2.- Example with a stained glass sample 43
CHAPTER 5: CHARACTERIZATION OF THE MODIFICATIONS THAT LASER TREATMENTS INDUCE IN STAINED GLASS 46
CONCLUSIONS 54
REFERENCES 57

LIST OF FIGURES

Fig. 1.1.1 Schematic representation of a grisaille paint layer 4
Fig. 1.2.1 A simplified mechanism of the corrosion of glass 10
Fig. 1.3.1 Representation of energy redistribution in laser-material interaction 17
Fig. 2.1.1 Left: photograph of the ultraviolet laser system; Right: calibration curves of laser power against frequency for different electric current intensities 21
Fig. 2.1.2 Left: photograph of the near-infrared laser system; Right: calibration curves of laser power against frequency for different electric current intensities 22
Fig. 2.2.1 Different scanning strategies adopted in this study 23
Fig. 2.4.1 Photographs of the stained glass sample 26
Fig. 2.4.2 Photograph of the commercial modern glass samples 27
Fig. 3.1.1 Photograph of the bottle after laser treatment 29
Fig. 3.1.2 Images obtained with confocal microscope of irradiation regions 30
Fig. 3.1.3 Image obtained with confocal microscope of irradiation region 10 30
Fig. 3.1.4 Images obtained with confocal microscope of irradiation regions 31
Fig. 3.1.5 Image obtained with confocal microscope of irradiation region 6 31
Fig. 3.2.1 Photograph of the transparent glass recipent after laser treatment 32
Fig. 3.2.2 Images obtained with confocal microscope of irradiation regions 33
Fig. 3.2.3 Images obtained with confocal microscope of irradiation regions 34
Fig. 3.2.4 Images obtained with confocal microscope of irradiated regions treated using the lowest fluence value with 1 pass (a) or 5 passes (b) 34
Fig. 3.2.5 Confocal images showing the topography of the two images presented in Fig. 3.2.4. 35
Fig. 3.3.1 Photographs of both industrial glass samples showing the effect of the n-IR laser 36
Fig. 3.4.1 Scratched window glass after being treated with a CO_2 laser 36
Fig. 4.1.1. Exemplary black and white image, which defines the bitmap scanning 38
Fig. 4.1.2. Photographs of the transparent stained glass sample taken with optical microscope 38

Fig. 4.1.3. Images obtained with confocal microscope showing the topography of the irradiation region 39
Fig. 4.1.4 Selective removal of black paint from glass 41
Fig. 4.1.5. Photograph of the aluminum foil under the glass after laser treatment 42
Fig. 4.2.1 Optical microscopic images showing the surface morphology of the sample after different number of laser passes 44
Fig. 4.2.2 SEM images showing the surface morphology of the sample after different number of laser passes 45
Fig. 5.1.1 A small corner fragment was cut from the stained glass sample 46
Fig. 5.1.2 Photographs of the corner fragment taken with optical microscope 47
Fig. 5.1.3 Image taken with FESEM of the irradiation regions I and II 48
Fig. 5.1.4 Higher magnification FESEM images of each zone 51
Fig. 5.1.5 Images taken with FESEM of the irradiation region I zone 6 showing the defects created on the glass surface 52
Fig. 5.1.6 Images taken with FESEM of the irradiation region III 52
Fig. 5.1.7 Images taken with FESEM of the irradiation region IV 53

LIST OF TABLES

Table 3.1 Parameters used in the laser treatments performed on irradiation regions ..29
Table 3.2 Parameters used in the laser treatments performed on irradiation regions ..33
Table 4.1 Parameters used in the selective laser cleaning performed on stained glass sample 44
Table 5.1 Parameters used in the laser treatments performed on irradiation regions I-IV.....47
Table 5.2 Results of EDS analysis for irradiation regions I and II (at%) 49
Table 5.3 Results of EDS analysis for irradiation region I zone 3 (at%).....51
Table 5.4 Results of EDS analysis for irradiation region I zone 6 (at%).....52
Table 5.5 Results of EDS analysis for irradiation region III (at%).....52

ABSTRACT

In this work, an attempt is made to go a step further in application of laser technologies in the restauration of stained glass. Several cleaning experiments have been conducted by two sub-nanosecond pulsed lasers (a UV laser and a n-IR laser), and materials taken for this study were a 16^{th} century stained glass sample from the Cathedral of Cuenca and some samples of commercial modern glass. Parameters affecting the cleaning outcomes were studied and the applicability of the selective cleaning method for stained glass restoration was explored. The treated samples were analyzed by optical microscopy, confocal microscopy, scanning electron microscopy and energy dispersive X-ray spectroscopy. Results showed that the alteration and ablation phenomena varied considerably depending on the selected laser parameters, as well as on the chemical compositions (thus also the colors) of the glass samples. Selective laser cleaning proves to be a feasible technique for relatively precise and controllable cleaning of cultural heritage stained glass, but caution must be taken in its application.

RESUMO

Aplicação de tecnologias laser no restauro de vitrais

Neste trabalho, tenta-se dar um passo adiante na aplicação de tecnologias laser na restauração de vitrais. Vários experimentos de limpeza foram conduzidos por dois lasers subnanosegundos pulsados (um laser UV e um laser n-IR), e os materiais tomados para este estudo foram uma amostra de vidro colorido do século XVI da Catedral de Cuenca e algumas amostras de vidro comercial moderno. Parâmetros afetando os resultados de limpeza foram estudados e a aplicabilidade do método seletivo de limpeza para restauração de vitrais foi explorada. As amostras tratadas foram analisadas por microscopia ótica, microscopia confocal, microscopia eletrônica de varredura e espectroscopia de energia dispersiva de raios-X. Os resultados mostraram que os fenômenos de alteração e ablação variavam consideravelmente, dependendo dos parâmetros do laser selecionados, bem como das composições químicas (e também das cores) das amostras de vidro. A limpeza seletiva a laser demonstra ser uma técnica viável para a limpeza relativamente precisa e controlável de vitrais do patrimônio cultural, mas deve-se tomar cuidado em sua aplicação.

AIMS AND OBJECTIVES

The cleaning process for stained glass has to consider the effectiveness of the treatment but also the potential damage for the substrate. In the last two decades, some studies of laser cleaning applied for stained glass windows have been performed and promising results have been obtained. However, it is important to explore if the new developments in laser technology can be used to overcome the problems that limit its application in the restauration of stained glass. Nowadays, it is possible to combine an ultrashort pulse laser with a galvanometric mirror scanner system which provides precision and reproducible scanning of the laser beam on the sample surface. This is the laser system used in this study. In this work selective laser cleaning will be performed on stained glass to determine the feasibility of picosecond lasers for glass restoration.

The main purposes of this study are to:

- revise bibliography about stained glass history, fabrication, deterioration and restoration;
- investigate the influence of relevant parameters in laser cleaning;
- conduct experimental research on selective laser cleaning of crust and deposit present on stained glass, and explore the applicability of the cleaning method for stained glass restoration;
- analyze the modifications that laser treatments induce in cultural heritage stained glass.

CHAPTER 1: LASERS IN STAINED GLASS RESTAURATION

1.1.- Stained glass windows

Stained glass windows are composed of shaped pieces of colored glass, held together in a lead network and enhanced with the surface application of a painted pigment (Bernardi et al., 2006; Brown and Strobl, 2002; Romich et al., 2003). Serving as light filters and iconographic supports, the stained glass windows are a critical element both in the religious and secular architecture (Basso et al., 2009).

1.1.1.- Materials and fabrication techniques

Colored glass pieces

It is obvious that the predominant component of a stained glass window is glass (Brown and Strobl, 2002). Most of what is known about ancient colored glass manufacturing technology stems from a medieval technical manual. A Benedictine monk named Theophilus wrote a manuscript entitled *De diversis artibus* (*On Divers Arts*) around 1100, in which he described the full process to make sheets of colored glass and to fabricate a window (Kleiner Fred, 2014). According to the author, materials for making ancient glasses were washed river sand (which is silica) and beechwood ash (which is potash, an alkali). The ingredients were mixed together in clay pots and then placed in a furnace, heated "for a night and a day". The heating and fusing of these materials combine them together to form liquid glass (Raguin, 2013; Schalm et al., 2007). Another glassmaking text, found in the work entitled *De artibus romanorum* (or *De colouribus et artibus romanorum*), advised the addition of powdered metallic oxides to the ash and sand to produce different colors of glass. The text was attributed to a monk Heraclius who presumably lived in the thirteenth century (Benton, 2009; Charleston, 1960; Royce-Roll, 1994).

Although the process of making stained glass has evolved both regionally and over time, the basic steps and main ingredients remain unchanged. These ingredients include silica, alkali fluxes and often metallic salts (coloring agent). Silica, which

forms the vitreous network of glass, requires a very high temperature in order to melt. So, alkali was introduced as the flux to decrease the melting temperature. The fluxes were either plant-based (beech or fern ash) or mineral-based (natron) and, depending on the nature of the material, enriched either in potash or in soda (Raguin, 2013; Weaver et al., 2016). The color was achieved by the addition of various metallic oxides during the fusing process: cobalt makes blue; copper makes red; lead or chromium makes yellow; chromium or copper makes green; manganese or nickel makes violet; and iron or manganese makes brown or black. Meanwhile, the firing atmosphere should be controlled because the redox condition of the atmosphere in the furnace chamber also influences the color produced (Raguin, 1988; Royce-Roll, 1994; Sterpenich and Libourel, 2001).

This kind of stained glass is additionally referred to as pot metal glass, the word "metal" is used due to the coloring metallic oxides added to the "pots" that held the melted glass (Benton, 2009). The pot metal glasses were more or less colored throughout with a single color. To create two colors on a single piece, or to retain the translucency in glass that contains strong light absorbing colorants, artisans began to exploit double-layered, or flashed, glass in the fourteenth century (Brown and Strobl, 2002; Marks, 2006). Flashed glass was produced by fusing a thin, concentrated layer of a previously colored glass onto the surface of another piece of clear glass or colored glass of a different hue (Benton, 2009). After cooling, the surface colored layer can be abraded away or acid-etched to reveal the color of the base (Raguin, 1988; Raguin, 2013). A typical example is ruby glass. The surface of the glass is coated with a thin layer of ruby (red) and the base is white, pale yellow, grey or green according to the required tint (Maurice Drake, 1928; Van der Snickt et al., 2016).

Traditionally, there were two major methods to form sheets of glass. The first method was called the crown method. In the process a bubble was blown from a globule of molten glass and transferred from the blowpipe to an iron pontil. The

glassblower then held the glass bubble in front of the glory hole of the furnace and opened it up by twirling or spinning. With continuous spinning the material would form a flattish circular disc as a result of the centrifugal force. The piece in the center with the mark where the pontil was attached was called the “crown”, giving the name to this technique (Malcom, 1990). The glass produced by this method tended to be relatively heavy and thick. The second method was called the cylinder, or muff, technique. In this method, the molten glass was blown into the shape of a long cylinder, the ends of which were pinched off. It was then reheated and cut lengthways with a hot iron. The heat caused the glass to relax and in the kiln it would be opened out to form a flat rectangle sheet. The resulting sheets were lighter, thinner, and usually larger than those produced by the crown method (Raguin, 1988; Raguin, 2013; Vilarigues et al., 2011). Whichever process was used, it is essential to place the finished flat sheet in an annealing furnace to cool it slowly, since the glass cracks if subjected to sudden temperature changes (Marks, 2006; San Casciani, 1989).

The discs or sheets of glass that were yielded by these techniques needed to be cut to the shapes required for incorporation into a panel of stained glass window. Medieval artisans shaped the glass pieces with a hot iron tool. They ran the hot iron along the proposed line of fracture slowly, followed by tracing the pattern with a cooler element, such as water or saliva, thus causing the glass to crack along the line. Then they snapped or broke the glass into shape. The roughly shaped edges can be trimmed by nibbling bits of glass off the rim with a hook-shaped metal tool (called a grozing iron) (Arnold, 2014; Kibler and Zinn, 2017; Raguin, 2013). The diamond tip cutter, which allowed for more precise cutting, began to replace the hot iron in the fourteenth century, and has in its turn been superseded by the modern glasscutter in the seventeenth century (Benton, 2009; San Casciani, 1989; Wigelsworth, 2006).

Painting on Glass

Once the necessary pieces of colored glass had been created, the painting took place. Most of the stained glass from the medieval and Renaissance periods were painted (Raguin, 2013; Wigelsworth, 2006). Three different kinds of glass paints can be distinguished. Grisaille has been used to color glass panes in shades of gray and brown since the ninth century. Silver stain was introduced to color glass in bright yellow in the early fourteenth century. Finally, various colored enamel paints were developed in the sixteenth century. Since then, many colors could be painted on a single glass piece (Benton, 2009; Schalm et al., 2009).

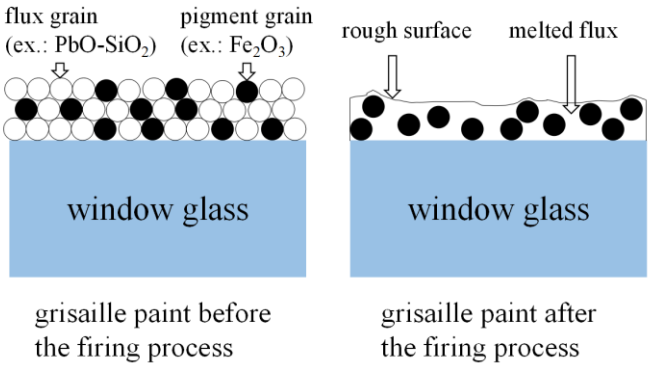

Fig. 1.1.1 Schematic representation of a grisaille paint layer (Schalm et al., 2003)

The grisaille (French for "greyness") is brownish or blackish vitreous paint used for indicating the details of faces, drapery folds, or background patterns, usually on the interior side of the stained glass windows (Hall, 2007; Kibler and Zinn, 2017; Raguin, 1988). It can be applied either as a thick, opaque line or as a thin, uniform layer. The grisaille paint was made from powders of finely ground lead silicate glass (fusible at a lower temperature compared with the substrate) mixed in the right proportions with pigments (metallic oxides) and organic binding agents. This mixture was usually applied with paint brushes. To affix the grisaille paint, the glass pieces had to be fired in a furnace at temperatures below the transition temperature of the substrate glass. The lead glass grains melt during firing and bonded the pigment grains to the base glass (Becherini et al., 2008; Benton, 2009;

Carmona et al., 2006; Schalm et al., 2003; Schalm et al., 2009). A schematic representation of the grisaille glass paint is shown in Fig. 1.1.1

Silver stain, also called yellow stain, is the only true staining method in stained glass. Glass artisans adopted this technique to achieve a permanent yellow color, which was used widely to color hair, drapery and small details of clothing. The staining method considerably decreased the need to cut and join small pieces of different colored glass together with lead strips. This technique involves, first, applying silver compounds in a carrier medium (such as clay or ochre) onto the exterior surface of the glass. Next, heating the glass panels at temperatures below the glass softening range (Kibler and Zinn, 2017; Raguin, 2013). The heating process allows silver ions to penetrate into the substrate glass, exchange with the alkali ions in the glass, and be reduced to metallic silver if they react with other metastable ions (such as Fe^{2+}, As^{3+} and Sb^{3+}) or non-bridging oxygens, which serve as electron donors (Fernandes et al., 2008; Findakly, 1985). Metallic silver aggregates precipitate as spherical metallic particles. After heating, the carrier medium is removed from the glass, revealing the characteristic yellow color produced by silver particles. The stain process can create a range of hue from lemon yellow to fiery orange, depending on the composition of the base glass, and the number, shape, particle size and its distribution of the silver particles (Jembrih-Simbürger et al., 2002). Silver stain could also be used to create the green color when it is applied onto blue glass (Brown and Strobl, 2002).

Enamel is a vitreous paint created from powdered glass and colored metallic oxides. The introduction of various colored enamels in the sixteenth century was a significant development in stained glass window technology. Since a vast range of colors could now be painted on a single glass piece, windows were no longer composed of small pieces of glass, each possessing its own individual color, but were made of larger pieces of light-colored glass treated as a painter's canvas (Benton, 2009; Campbell, 2006). The enamel paints were typically prepared by

melting together a flux (a powdered, low melting lead glass) with a coloring substance (metallic oxide). The molten glass was quickly cooled down and ground into a fine powder, then mixed with a sticky medium such as water-based gum or oil in order to obtain a paste paint that can be applied onto a glass pane. The painted glass was subsequently fired and cooled slowly. The enamel transformed into a thin homogeneous glass layer which adhered to the substrate and turned a transparent color during the process (Attard-Montalto and Shortland, 2015; Jones and Matthews-Jones, 2016; Schalm et al., 2009).

Lead cames and metal framework

The second major structural element in a stained glass window is lead. The fired pieces of glass were joined together with flexible strips of lead commonly called "cames". In the Middle Ages, lead cames were cast in molds. From the late sixteenth century, cames were made by extruding the lead through a mill (Brown and Strobl, 2002; Raguin, 2013). The H-shaped lead cames were grooved on either side to accommodate the edges of the inserted glass pieces. The lead between the pieces of glass is thinner and has wider flanges in late windows than in early windows (Benton, 2009). Joints of the lead cames were soldered on both sides and putties were forced between the glass and came flange to make a watertight seal. In addition to holding the assembled pieces of glass together, the lead also separated the colors and formed an integral part of the design (Hall, 2007; Kibler and Zinn, 2017; Kleiner Fred, 2014). The completed panel was placed into a metal framework which was referred to as an armature, and then fixed into the window opening. Additional reinforcement was provided by iron bars and stone tracery. An iron bar grid set in the frame was used to give the panel structural rigidity. The iron bars might also be curved to follow the major shapes in the panel so as not to diminish its designed effect. Stone bar or rib supports called tracery were often used on large circular windows (Benton, 2009; Raguin, 1988; Raguin, 2013; San Casciani, 1989).

1.1.2.- Producing a window from start to finish

A stained glass window is created through the collaborative efforts of artisans with different skills (Brown and Strobl, 2002). First, the sketch was drawn full scale by a master designer on a large wooden panel, indicating the exact sizes and shapes of the separate pieces and noting the colors for each region. The design must include some allowance for the thickness of the lead cames (Benton, 2009; Kleiner Fred, 2014). When larger windows were used, the first design would be drawn at a smaller size and then enlarged to a full-scale rendering. Then colored glass sheets were provided by glassblowers and the individual pieces were cut by glassworkers to the required size and shape. Next, painters added details by tracing the design on the wood board through the colored glass. The painted glasses were then heated in a kiln to fuse the paint to the surface (Raguin, 2013). Finally, the glaziers joined the pieces of glass by strips of lead and strengthened the completed window with an iron framework (Kleiner Fred, 2014).

Every component of the stained glass window may yield precious information about the past. When implementing a conservation program, it is required that as much of the original historic fabric as possible is preserved, and all aspects of the window should be taken care of (Brown and Strobl, 2002). Inappropriate repairs and maintenance would induce further deterioration and ultimately result in the loss of heritage significance of the window (Wong, 2016). Repairs can only be carried out after a careful evaluation of the condition of the stained glass window has been performed (Vogel and Achilles, 1993a).

1.2.- Pathologies and restoration methods

1.2.1.- Pathologies

Since their creation, stained glass windows are prone to deterioration due to unfavorable environmental conditions. Three elements of the stained glass

windows are susceptible to deterioration: the colored glass itself; the applied paint; and the skeletal structure that holds the glass (Vogel and Achilles, 1993a).

Glass

Glass is the typically brittle material, and its composition makes it highly sensitive to moisture and to atmospheric pollution (Brown and Strobl, 2002). The weathering of stained glass pieces does appear as a consequence of the synergic effect of atmospheric agents and humidity (Carmona et al., 2006). Other factors that contribute to the deterioration process include changes in temperature, microorganisms, meteorological and human induced hazards, and intrinsic factors such as glass impurities and tiny internal fractures. Glass is also quite vulnerable to scratching, cracking or breakage (Godoi et al., 2006; Vogel and Achilles, 1993a).

Crack, breakage and the methods of repair

One of the most common causes of crack or breakage is physical impact. Cracked or missing stained glass pieces are possibly caused by accidents, intentional acts of vandalism, and the failure of lead cames. Cracks can also result from internal stress generated by improper annealing. Windows assembled with long, narrow and angular glass pieces are inherently susceptible to cracking (Wong, 2016). The cause of the cracks can be diagnosed by the crack paths: impact-related cracks typically radiate away from the impact source. Stress cracks caused by inadequate annealing will travel a highly irregular path. When the window is subject to temperature-induced expansion and contraction, mechanical vibration or other stress, the cracks will extend as the contacting glass edges rub against each other. It is, therefore, important to repair cracks in important areas as soon as the fine cracks are detected. Traditionally, cracks were repaired with a “false lead”, a lead flange spliced over a fine crack. Even though the lead conceals the crack, it creates a greater degree of visual intrusion and provides no true bond to the glass (Vogel and Achilles, 1993b). Today, there are two primary types of repair to consider: chemical repair (epoxy glue and silicone glue) and mechanical repair (copper foil)

(Wong, 2016). These methods differ from each other in strength, visual effect and reversibility, and the appropriate technique should be determined on a case-by-case basis (Vogel and Achilles, 1993a).

Copper foil is generally the best option for less significant areas. The thin copper tape can produce a strong repair when it is applied along each side of the glass break and soldered. Copper foil has a negligible aesthetic impact and is totally reversible. Since heat is required, this kind of repair is not appropriate for unstable glass. Epoxy glue is often used in important painted areas. The synthetic, colorless adhesive produces a very strong repair and can even be tinted to improve the legibility of the stained glass (Raguin, 1988; Wong, 2016). The drawback of epoxy glue is that it is the least reversible of these techniques and will deteriorate in sunlight. In contrast, silicone glue is easily reversible and not affected by UV light, temperature or humidity. But this repair method has the lowest strength and is easily detectable because silicone refracts light differently from glass (Vogel and Achilles, 1993a).

Original glass should be retained and preserved wherever possible, but sometimes the only option is to replace the broken or missing glass. Replacement glass should closely match the existing pieces with the support of evidence and records. To prevent any confusion in the future, the new glass pieces should be scribed at an inconspicuous position (such as the edge under the came) with the date (Vogel and Achilles, 1993a; Wong, 2016).

Dirt and corrosion

A variety of degradation phenomena take place on the stained glass windows (Römich and Weinmann, 2000). Dirt, grime and soot can build up on the stained glass from pollution and smoke. The use of incense or candles in churches can deposit carbon layers on the glass. All these deposits can substantially reduce the

amount of light passing through the windows and make them muted and lifeless (Vogel and Achilles, 1993a).

Corrosion (weathering) of glass may be the result of the attack by water (humidity, rain), chemicals (acidic pollutants), or possibly biological agents (Römich et al., 2003; Raguin, 1988). In addition, glass composition and previous restoration campaigns may also influence the weathering process (Murcia-Mascarós et al., 2008; Römich and Weinmann, 2000). Generally, a 3-stage system can be established between the ambient atmosphere, the adsorbed water layer and the original glass surface (Godoi et al., 2006; WoisetschlaÈger et al., 2000). Fig. 1.2.1 presents a simplified mechanism for the corrosion process.

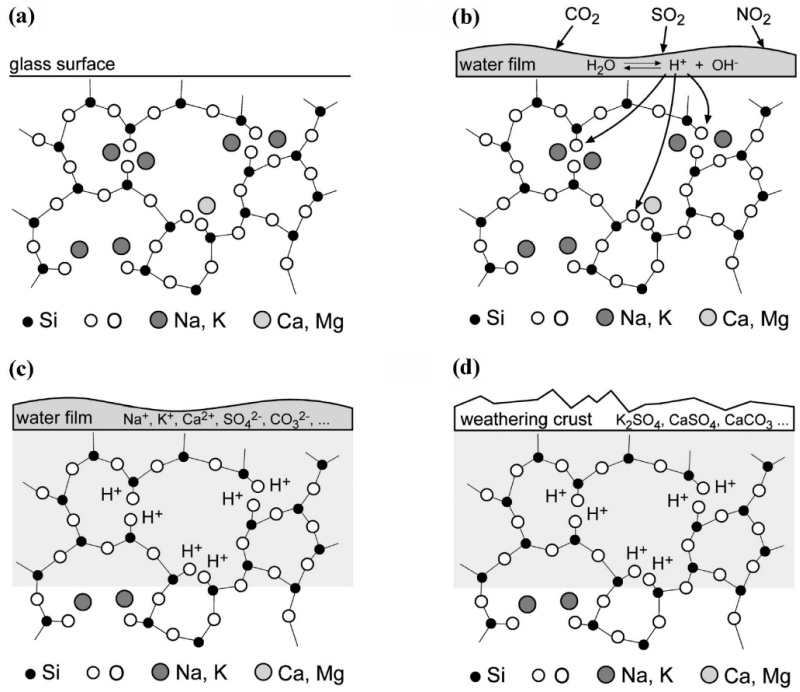

Fig. 1.2.1 A simplified mechanism of the corrosion of glass (Melcher et al., 2010)
(a) Glass corrosion starts with a clean and unweathered surface. (b) A water film is adsorbed on the glass surface, enabling the exchange of ions between the ions (H^+) from water and the alkaline ions (K^+ and Ca^{2+}) of the glass, which may be enhanced by the presence of acidifying gases. (c) A leached and hydrogen-enriched layer is formed. (d) Corrosion products remain on the surface of the glass after the water evaporates.

As can be seen from Fig. 1.2.1, a thin water film formed on the glass surface enables an ion exchange process, where the modified cations (K^+ and Ca^{2+}) in glass network

are leached out and the hydrogen bearing species from water are incorporated into the silicate structure. Atmospheric pollutants or airborne particulate matters can dissolve in the water layer, leading to a reduction in its pH and an enhanced diffusion of ions. If the product of the concentrations of respective ions exceeds the solubility product of a specific compound, precipitation of this corrosion product takes place (Godoi et al., 2006; WoisetschlaÈger et al., 2000). After the water film evaporates, the corrosion products remain on the glass surface. Their chemical compositions significantly depend on the composition of the glass and the type of the atmospheric pollutants (Melcher et al., 2010). Most of the reported composition of the crusts developed on stained glass windows consists of silica, SO_3, CaO and K_2O. Salts with poor solubility which darken the glass are mainly hydrated silica ($SiO_2 \cdot nH_2O$), gypsum ($CaSO_4 \cdot 2H_2O$), basanite ($CaSO_4 \cdot 1/2H_2O$), arcanite (K_2SO_4), syngenite ($K_2Ca(SO_4)_2 \cdot H_2O$), palmierite ($K_2Pb(SO_4)_2$), anglesite ($PbSO_4$) and calcite ($CaCO_3$). Soluble nitrates and other soluble carbonates and sulphates do not form crusts. Crusts consisting of $CaCO_3$, $CaSO_4$ or $PbSO_4$ can also develop on grisailles (Murcia-Mascarós et al., 2008).

Biodeterioration

As mentioned above, another important factor that enhance corrosion is biodeterioration. The biodeterioration processes on glass happen as the result of the metabolic activities of microbial communities composed mainly of lichens, bacteria and fungi (Marvasi et al., 2009; Schabereiter-Gurtner et al., 2001). The role of microbial communities in the degradation of glass includes both mechanical and chemical destruction. The filamentous growth of fungi and some actinobacteria can cause a mechanical destruction. The adsorption of water could create a leaching environment, enhancing the chemical destruction of the glass. Organic or inorganic acids secreted by microorganisms can cause changes in pH, the leaching of elements from glass and the chelation of special glass components. In summary, biological activity on glass surfaces causes several types of damage, including cracks,

corrosion, biopitting and patina formation (Drewello and Weissmann, 1997; Krumbein et al., 1991; Piñar et al., 2013).

1.2.2.- Restoration methods

Glass cleaning

Depending on the state of conservation, the stained glass window is either dismantled or cleaned and repaired in-situ. The cleaning process is one of the most delicate phases of the restoration-conservation work of stained glass. Both slightly-adhered debris and strongly-fixed crusts should be removed from the glass surface to restore the windows' original iconography and to prevent further deterioration and alteration (Vogel and Achilles, 1993a). Currently, the cleaning of glass surfaces is achieved through various mechanical and chemical methods. The mechanical methods range from bristle brushes to glass-fibre brushes and scalpels. Chemical cleaning methods commonly include the use of water or organic solutions (Delgado, 2016). The choice of cleaning methods and agents depends on the type of deterioration observed, and whether the window has to be dismantled or not. The least adhered debris can be removed using non-destructive brush. The strongly fixed deposits need to be removed using carefully selected chemical cleaning methods (Murcia-Mascarós et al., 2008). Water alone should be tried first (distilled water is preferable) when cleaning dirt from glass. For the removal of shellac, lacquer, or very stubborn grime, alcohol or organic solvents may be required and must be used only when gentler methods have failed. Aggressive or caustic cleaners, or solutions with pH values in the acidic range or alkaline range should never be used in the cleaning process (Vogel and Achilles, 1993a; Wong, 2016).

Before starting any cleaning work in painted areas, the paint applied to glass should be inspected to make sure it is firmly attached and will not be removed. The loss of paint would cause irreversible damage to the artistic integrity of the stained glass window. The method that shows a high efficiency in removing the dirt or

diminishing the crusts may not be the best one to use because it may also induce damage or long-term risks to the glass or the paint layer (Raguin, 1988).

It is also very important that rather than removing the corrosion deposits down to the bulk glass, the leached glass surface layer (gel layer) belonging to the original substance should remain unaltered during cleaning. The gel layer can protect the glass beneath from further degradation. The same requirement applies to the removal of the bio-layer, which are the result of the microbial metabolism on the glass surface (Delgado, 2016; Römich et al., 2003).

Deterioration and restoration of glass paints

In some cases, glass weathering can cause the alteration of the adhering paint. In other cases the paint itself may deteriorate. Two forms of degradation can be distinguished: degradation can appear as disintegration and pulverization of the glass paint, or areas of paint may maintain internal cohesion but peel or flake off the substrate due to loss of adhesion (Carmona et al., 2009). Two mechanisms govern the deterioration phenomena of glass paint: a chemical mechanism including the corrosion and pulverization of the paint, and a physical mechanism associated with micro-fractures (Becherini et al., 2008). As mentioned previously, the glass piece is again heated in a kiln after the paint is applied. If the firing is improper or the composition of the paint is not appropriate, tensions will arise, leading to detachment of the glass paint (Murcia-Mascarós et al., 2008). Paint failure is commonly caused by incomplete firing (baking the glass either for too little time or at too low a temperature). Some chemical compositions of historical glass paints appear to be unstable. For example the enamels with a high content of K_2O and a low content of PbO and CaO show a relatively fast deterioration (Schalm et al., 2009). Improper steps in the painting process can also produce fragile paint. For instance, the paint may not fuse properly if it is poorly mixed or applied too thick to the glass (Vogel and Achilles, 1993a). In addition to the degradation due to material properties or

manufacturing and painting processes, paint on glass is extremely vulnerable to the effects of condensation (Carmona et al., 2009).

Several paint treatments and surface coatings have been developed to consolidate and protect deteriorated paint. Historically, natural wax has been used to achieve the consolidation of unstable paint in some cathedrals (Carroll et al., 1994). In contemporary restoration practices, Paraloid B72 is most commonly used for this application due to its good reversibility. But as an organic material, Paraloid B72 is subject to the environmental impact with time, and thus its long-term stability is limited. In recent years, new materials like sol–gel based consolidants have been proposed for the consolidation of paint on stained glass and received attention by the expert community due to their promising laboratory results (Carmona et al., 2009). If serious paint failure occurs in a prominent area of the window, a coverplate of thin, transparent glass can be painted on the backside with the reverse image of the missing features and placed over the original. The coverplates should be mechanically attached to the window, rather than laminated, so they can be removed easily later if necessary (Vogel and Achilles, 1993a).

Deterioration and restoration of the skeletal structure

Another common threat to stained glass windows is deterioration of the skeletal structure. The structure consists of frame members such as metal frames or stone traceries that provide structural rigidity to the glass panels, and assembly materials such as lead cames that hold the pieces of glass together. Metal frames and saddle bars can corrode over time and quicken the deterioration of the glazing and sealants. Stone traceries can fracture and spall, which contributes to structural failure of the window. Maintenance of the frame members at regular intervals is necessary to prevent further deterioration. This involves regular caulking and periodic reglazing. Deteriorated frames should be repaired where necessary by removing the degraded sections and splicing in new ones. Stained glass windows should only be dismantled when they need to be flattened, reputtied, reinforced, or releaded.

Occasionally, leading patterns was designed with inadequate bracing, this also results in structural failure (Vogel and Achilles, 1993a). In other cases, the arrangement of support is adequate, but the solder joints may be weak and fractured, and the putty may be deteriorated or have fallen out from under the lead flange (Raguin, 1988; Wong, 2016). When the panel loses stability, there is a chance the stained glass could sag, bulge and eventually even fall out from vibration or wind pressure. Windows should be removed from the opening and flattened with extreme care when the sagging and bulging has reached the precarious level. The flattening process also provides a good opportunity to resolder the joints and reputty the windows. Lead cames are subject to corrosion from moisture and humidity, and fatigue failures associated with thermal expansion and contraction (Sloan, 1991). As an integral component of the stained glass window, the lead came should only be replaced if it is exhausted beyond repair. Releading a window is very time consuming and expensive. The individual pieces of glass need to be removed from the lead cames, the old putty needs to be cleaned from each glass piece, and then all the pieces need to be rejoined accurately. It is essential to retain the historical accuracy by following the lines, profile and width on the rubbing of the original leadwork (Vogel and Achilles, 1993a; Wong, 2016).

1.3.- Laser cleaning

1.3.1.- Laser cleaning in conservation

Research on the topic of laser cleaning in conservation began in the 1970s, when John F. Asmus performed a series of studies on the use of lasers in cleaning altered marble, metal, and terracotta (Asmus et al., 1973). Asmus's experiments revealed practical applications of the novel approach and its possible future developments. However, laser cleaning did not experience a widespread growth in the field of artwork conservation because of the technological limits and high costs at that time. The performance of laser devices increased markedly during the eighties. But the costs remained high and the productivity gap between laser cleaning and traditional

cleaning techniques was large. In this context, conservation community did not realize the full potential of this new cleaning technology (Siano, 2008). In the early nineties the situation drastically changed as a result of successful collaborations between research institutes and continuous support from European Framework Program together with various national program for the development of new methodologies and technologies for the conservation of cultural heritage. In the UK, M. I. Cooper and D. C. Emmony with the conservation support of J. Larson, conducted detailed experimental investigations on the use of laser cleaning to preserve limestone and marble sculpture (Cooper and Larson, 1996; Cooper et al., 1995). D. C. Emmony and P. Pouli have also investigated laser-induced discoloration effects on medieval pigments (Pouli et al., 2001). During 1992-1995, led by Dickmann at the Lasercenter Fachhochschule Münster and Römich at the Fraunhofer-Institut für Silicatforschung in Germany, two independent feasibility studies were carried out on laser removal of organic and inorganic corrosion from stained glass (Romich et al., 2003). Their work played a crucial role in the further development of the field (Fotakis et al., 2006). In 1995, an international conference on lasers in the conservation of artworks (LACONA) was held in Crete, Greece. For the first time restorers and scientists were brought together to discuss the potential of lasers in art conservation. Since then this field has gained enormously in importance. The creation of LACONA and subsequent ten LACONA gatherings, held every two years, reveal signs of maturation of laser technology in the conservation field (Asmus, 2003; Nimmrichter et al., Sept. 21–25, 2005).

1.3.2.- Principles of laser conservation

The word LASER is an acronym termed Light Amplification by Stimulated Emission of Radiation. Because of the unique properties, such as monochromaticity, directionality and coherence, laser has been considered a technological advance in all its areas of application (Mahamood, 2018). When laser interacts with material surface, the incident radiation may be absorbed, transmitted, reflected and scattered (Pouli, 2000). The amount of each type of

energy is determined by the parameters of the laser radiation and absorption properties of the material. Scattering and absorption contribute to attenuation and spatial diffusion of the laser energy (Hrnjić, 2015). A qualitative representation of the energy redistribution in irradiated solids is shown in Fig. 1.3.1.

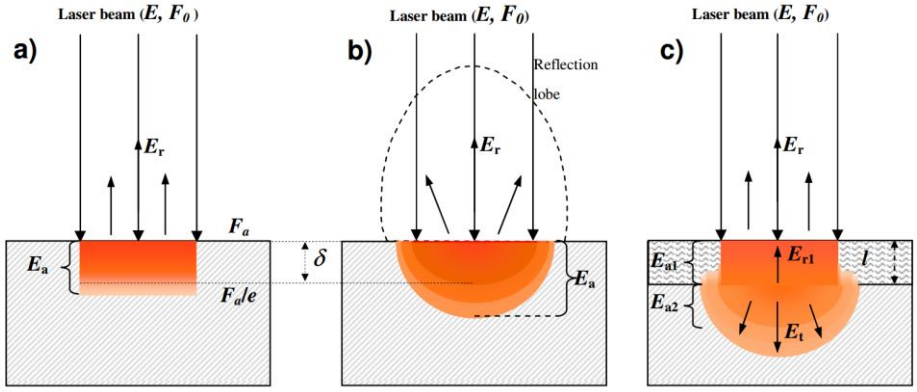

Fig. 1.3.1 Representation of energy redistribution in laser-material interaction (Siano, 2008)
(a) absorbing material; (b) diffusing material; (c) composite situation of an absorbing layer on a diffusing substrate (E_r, E_a = reflected and absorbed energies)

The absorption of laser radiation can lead to ablation, which is the main phenomenon involved in laser cleaning. Ablation involves the ejection of material from a laser irradiated surface, sometimes accompanied by the formation of a plasma when intense laser irradiation is used (Cooper, 1994). Three main types of interactions may occur during the process of laser ablation, which are photothermal, photochemical, and photomechanical interactions. The exact interaction mechanisms depend on the laser parameters and on the physical and chemical properties of the target material. The thermal properties of the material (i.e. thermal conductivity and heat capacity) are important parameters to evaluate both the volume of the material affected by laser irradiation and the maximum temperature reached in the process. Strong absorption of energy leads to rapid heating of the material, followed by its thermal expansion and the emission of a shock wave, which causes ablation at the surface (Koh, 2005). The minimum energy density required to achieve ablation is called the ablation threshold. When the ablation threshold of the material to be removed is lower than that of the original

substrate, the removal process can be performed within safe parameters. That is, the energy density deposited onto the sample surface is sufficient to clean the contaminants but not enough to damage the substrate material. The cleaning is described as a "self-limiting" process in this case (Hrnjić, 2015; Mateo et al., 2005).

1.3.3.- Laser cleaning parameters

When laser cleaning technique is employed to remove contaminants from the surfaces of artworks, proper parameters should be selected for efficient and safe cleaning. At low energy densities the laser irradiation may not be enough to completely remove contaminants. While the use of overly aggressive parameters can result in over cleaning and consequent damaging of the artefacts (Koh, 2005). This section discusses the main controllable parameters that can affect the performance of laser cleaning, including wavelength, pulse duration, energy density and so on.

An important parameter associated with laser cleaning is the wavelength of the laser system. As the reflectivity and absorption coefficient of contamination and substrate material varies with the wavelength of the incident laser, different wavelengths will result in different cleaning efficiencies. The choice of an appropriate wavelength is essential for effective cleaning. Generally, the wavelength that offers a higher absorptivity in the unwanted surface layer than in the underlying substrate is preferred (Hrnjić, 2015; Quintana, 2016).

Once the laser is activated, the emission of laser energy may be continuous (cw operation) or pulsed. A continuous wave laser emits a laser beam with a constant power and intensity over the entire time interval. Whereas, a pulsed laser generates laser pulses at varied rates, with an on time when energy is released (pulse duration or pulse width) and an off time when there is no energy released. When energy is emitted in very short time, it results in high peak powers and peak intensities, which is more suitable for ablation of materials. The laser pulse duration is another

important parameter affecting the performance of laser cleaning. In principle, the shorter the pulse duration, the higher the peak power intensity made available, and the stronger the shock wave generated in the process (Millis and Levine, 2013; Pradhan et al., 2017; Rea, 2004). With the development of laser technology, short pulse durations of nano (10^{-9}), pico (10^{-12}) or femto (10^{-15}) -second can be obtained (Fotakis et al., 2006). The ultrashort pulse laser offers several advantages. When its pulse duration is less than the thermal conduction time of the sample, ultrashort pulse laser can generate an almost non-thermal interaction in the ablation process, allowing precise and thermal-damage-free removal of material (Hrnjić, 2015; Hu et al., 2010; Kerse et al., 2016). Besides the single pulse effect, however, it is also important to take into account the cumulative heating effects from successive pulses, which would occur if the repetition rate (the number of emitted pulses per second) is too high to allow a complete thermal relaxation of the irradiated material within the time interval between two consecutive pulses (Siano, 2008; Siano and Salimbeni, 2001).

Once the correct wavelength and pulse width have been selected, laser fluence and irradiance, which play a central role in the ablation process, should be considered. Fluence, also referred to as energy density (Rubahn, 1999), is given by the following equation:

$$F = \frac{P}{f_{rep} A}$$

where P is the average output power of the laser, f_{rep} is the repetition rate and A is the spot area. It has to be noted here that the laser pulse duration is not involved in this equation, which could create some ambiguity when comparing fluence values of lasers with different pulse durations. When evaluating damage thresholds for laser cleaning, it is more appropriate to use irradiance, which is calculated as:

$$I = \frac{P}{f_{rep} A t_p} = \frac{F}{t_p}$$

where t_p is the pulse duration (Rodriguez-Navarro et al., 2003). Also, it is expected that using the same irradiance value will guarantee reproducible results in the treatment of artefacts (Hrnjić, 2015).

CHAPTER 2: EXPERIMENTAL METHODS

2.1.- Laser systems

2.1.1.- UV sub-nano laser

In this study two laser systems were used. The first one was an ultraviolet laser (Rofin-Sinar PowerLine Pico 10-355) with a wavelength of 355 nm. The maximum output power is 3 W and the laser was operated with a range of frequencies between 200 and 800 kHz. The diameter of the laser beam is 17 µm and the pulse duration is 300 ps. The laser power was controlled by changing the electric current from the power source. The UV laser system and the calibration curves of laser power against frequency for different electric current intensities are shown in Fig. 2.1.1, indicating that the maximum power is reached at 300 kHz.

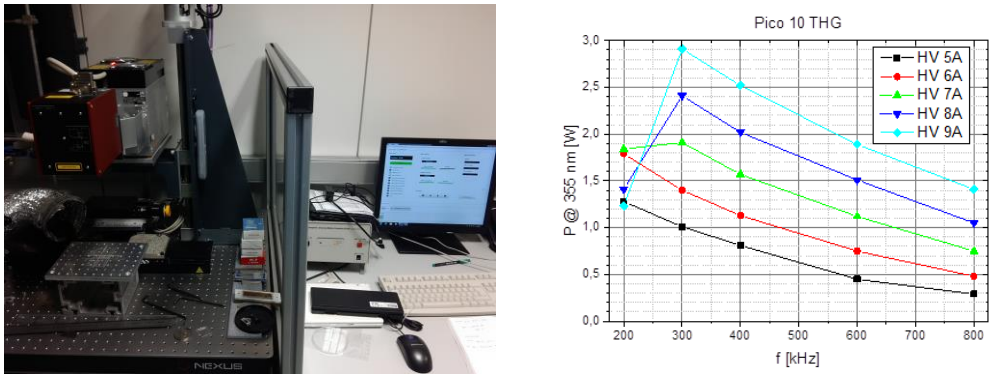

Fig. 2.1.1 Left: photograph of the ultraviolet laser system; Right: calibration curves of laser power against frequency for different electric current intensities

2.1.2.- n-IR sub-nano laser

The second laser system was a near-infrared laser (Rofin-Sinar PowerLine Pico 10-1064) with a wavelength of 1064 nm, a pulse duration of 800 ps and a maximum output power of 8 W. The pulse repetition rate can be modified between 200 and 800 kHz and the spot diameter of the laser beam is 25 µm. Fig. 2.1.2 shows the n-IR laser system and the calibration curves of this laser. In this case, at frequencies higher than 300 kHz the relations between the source current and the output power are the same.

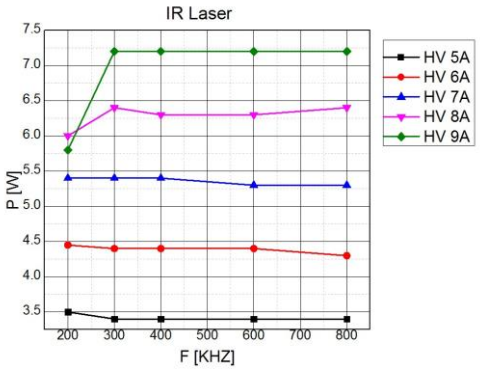

Fig. 2.1.2 Left: photograph of the near-infrared laser system; Right: calibration curves of laser power against frequency for different electric current intensities

2.2.- Modes in laser processing

Each laser system is combined with a galvanometric mirror scanner system, which provides precision scanning of the laser beam on the sample surface. Laser scanning parameters can be set by the laser system control software (Visual Laser Marker). It is also possible to upload a vector file or a bitmap image into the software to control the area where laser cleaning has to be carried out. In this work we have been working with three different modes of laser processing: continuous mode, burst mode and bitmap mode.

2.2.1.- Beam scanning, continuous mode

In the continuous scanning mode, the operator can select the frequency; the laser scanning speed and the distance between lines; and the system covers the surface uniformly. In addition, it is possible to control the scanning direction. When this protocol is used, it is important to have in mind that when the laser beam reaches the border of the irradiation region, it has to move its way back or start from the other side. In consequence, there is a region of the sample, where the scanning speed has been reduced until stopping the laser and where the treatment has been stronger. This can cause localized defects on the surface that can be very relevant in Cultural Heritage. If it is possible, the scanning has to be performed over areas higher than the sample size or to use some kind of masks or a shutter (Strassl et al., 2008). Also the scanning can be performed using a unidirectional or a bidirectional

configuration as it is observed in Fig. 2.2.1. In the bidirectional scanning pattern, the laser moves in a zigzag way across the sample surface. In the unidirectional one, the laser always starts from the same side of the irradiation region. Different scanning patterns would cause different phenomena. In the bidirectional case, it is important to consider that the laser starts a line in a region that is close to the region that has just processed at the end of the previous line, and that can be still hot (point A in Fig. 2.2.1(a)), increasing even more the effect of the laser on the border of the scanned area and the differences between center and border. By contrast, when the unidirectional configuration is used, the time between two equivalent position in two lines is the same in all the line and only the effects of stopping the laser have to be considered.

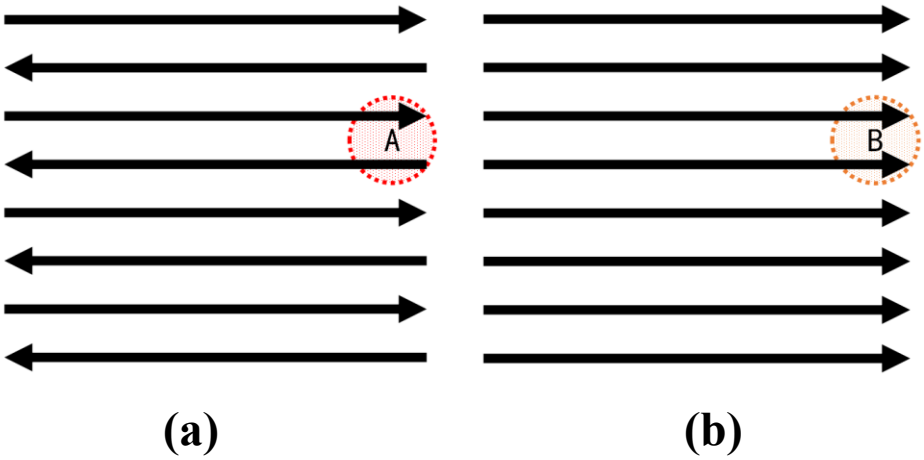

Fig. 2.2.1 Different scanning strategies adopted in this study
(a) bidirectional scanning; (b) unidirectional scanning

2.2.2.- Burst mode

The burst mode consists on a spot-by-spot scanning process with adjustable laser parameters. In burst mode, the laser system produces a sequence of a defined number of pulses (a burst) with a high intraburst repetition rate (Kerse et al., 2016). A single burst is incident at a given spot and the distance between the bursts can be set by software. It is also possible to adjust the number of pulses in a burst and the energy of each individual pulse, which would provide more flexibility and convenience in the cleaning process. This scanning process is slower than the

continuous one because the laser stops at every point.

2.2.3.- Bit-map mode

Bitmap mode is a mode for selective laser scanning, where the scanning is defined by a bitmap image uploaded into the control software for the laser system. Following the bitmap pattern, the irradiation will be performed spot by spot on the sample surface and the image resolution defines the number of pulses per area, and in consequence the strength of the laser treatment. But this is its main limitation because this is the only processing parameter that can be adjusted to control the process.

2.3.- Characterization techniques

2.3.1.- Confocal microscopy

A confocal microscope is a 3D optical profiler system that provides a good technique for obtaining sharp, high-resolution images of the topography of a surface. This type of microscope uses point illumination and with the help of a pinhole, most of the light from outside the microscope's focal plane is excluded from detection. The resulting images have significantly improved depth discrimination, higher lateral resolution and better contrast than those of a conventional microscope. Furthermore, confocal microscope can be used to generate three-dimensional images of a volume of the surface morphology by assembling a series of thin optical sections taken along the vertical axis (Merkel et al., 2012; Seewig et al., 2013; Semwogerere and Weeks, 2005). These optical systems have some advantages over tactile profilometers. The measure is non-contact avoiding the possibility of damaging the surface. In addition it can be applied with transparent materials. In this study, a Sensofar PLμ2300 confocal microscope was used to investigate the surface morphology and topography of the samples. The equipment is equipped with four confocal objectives (x10, x20, x50 and x100) and two interferometric ones (x10, x20). The equipment is also equipped with a displacement table in order to

be able to obtain extended topographies.

2.3.2.- Portable optical microscopy

A portable optical microscopy (Dino-Lite Edge) was used to get rapid feedbacks relating to the surface alteration of the samples. The maximum magnification of this microscope is x230 and it has been used to obtain a fast initial characterization of the effects of the laser treatments.

2.3.3.- Scanning electron microscopy

The scanning electron microscope (SEM) can also be used to reveal surface morphological features of a specimen by scanning its surface with a focused electron beam. SEM images can be taken at a much higher resolution and depth of field than confocal microscopy images. However, the sample preparation is more challenging for standard SEM imaging because it requires having a conductive layer on the surface of the sample and, in some materials, as glasses, it requires to put a metal coating to reduce spatial charging. If SEM is combined with energy dispersive X-ray spectroscopy (EDS or EDX), chemical information can be obtained from the excited characteristic X-rays of the sample (Hrnjić, 2015; Jenness et al., 2008; Wirth, 2009).

Two SEM instruments were used in this work. A JEOL JSM 6360-LV scanning electron microscope was used for the characterization of the transparent stained glass sample. Its advantage is that it can work in the low vacuum mode which allows to analyze non-conductive samples without any previous preparation. The accelerating voltage of 15 kV was applied and the maximum resolution of the instrument in low vacuum mode is 4.0 nm.

A small piece of glass that was cut from the stained glass sample was carbon coated and analyzed using a Carl Zeiss MERLIN^{TM} high vacuum field emission scanning electron microscope (FESEM), coupled with EDS INCA 350 produced by Oxford

Instruments with energy resolution from 127 eV to 5.9 keV. Accelerating voltage used was in the range of 5 kV to 15 kV. In this equipment, high vacuum is required and a carbon coating in the glass surface was necessary to improve the imaging by creating a conductive layer on it.

2.4.- Materials

2.4.1.- Sample of historical stained glass

This work concerns the application of laser cleaning in the conservation of a 16th century transparent glass sample from stained glass windows of the Cathedral of Cuenca. The glass piece was removed from the window in the late 19th and early 20th century and stored in the archive of the cathedral since then. Fig. 2.4.1 shows the photographs of the two sides of this stained glass sample. It can be observed that the internal side of the glass sample is in a better state of conservation than the external side. Viewed from the internal side, feather-like patterns painted with grisaille can be recognized (Fig. 2.4.1(a)). Some small craters filled with whitish deposits could also be observed on this side. On the external side of the glass sample, it can be observed that many areas of edge portion were covered by a thick layer of yellowish crust. We consider that the crust could be attributed to residual deposits of putty and/or cementing materials used to fix the glass piece into lead cames. A detailed discussion of this point will be provided in chapter 5. Microbial colonization was not observed on this historic glass sample.

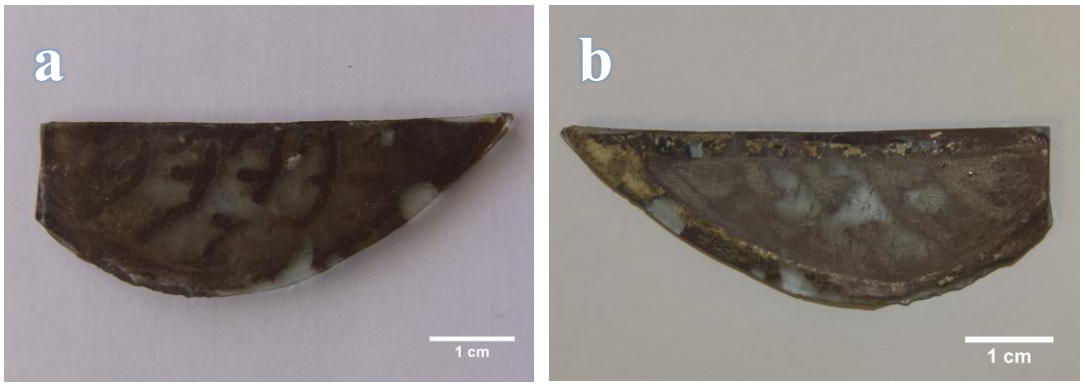

Fig. 2.4.1 Photographs of the stained glass sample: (a) internal side; (b) external side

It has been mentioned earlier that the grisaille is usually applied on the interior side of the stained glass windows. However, for this sample, the grisaille is located on its external surface. This may be due to a previous erroneous restoration, or the grisaille was originally fired on the external surface (Becherini et al., 2008). As can be seen in Fig. 2.4.1(b), several strongly adhered crusts were formed in painted areas on the external surface. Removing crusts from the glass sample in this case is correspondingly more challenging.

2.4.2.- Samples of commercial modern glass

The work was initiated with some commercial modern pieces of transparent and colored glasses. They are a beer bottle and a cosmetic recipient. These samples have been used to learn the use of the high power lasers and to define the range of conditions of the laser that can be used minimizing the possibilities of creating some defects on glass. In addition, some particular experiments have been performed on pieces of window glass and microscope slides.

Fig. 2.4.2 Photograph of the commercial modern glass samples

CHAPTER 3: IDENTIFICATION OF ABLATION THRESHOLD IN COMMERCIAL MODERN GLASS

Initially we performed some experiments in industrial glasses in order to explore the different kind of defects that the laser treatment can generate in the surface of the glass and to determine which laser parameters can be used without damaging the glass. We choose two different bottles of brown and transparent glass, with some commercial advertisements sticky on their surface.

It is important to have in mind that glass is a fragile material and the high thermal stresses that can be generated due to the localized high temperatures generated during the laser treatment can induce crack generation.

3.1.- Effect of using the UV laser to process brown industrial glass

First experiments were conducted to perform laser treatments directly on the glass. The laser has scanned areas of 12.5 mm^2 (5mm × 2.5mm) using a continuous bidirectional mode with a laser scan speed of 50 mm/s, a frequency of 300 kHz and a distance between scanning lines of 10 microns. We have chosen this frequency because with lower frequencies the pulse energy is higher and the ablation processes, which are relevant in the laser cleaning process, are more important. A set of experiments with increasing values of laser power has been performed. The spot fluence has varied from 1.47 J/cm^2 up to 3.52 J/cm^2, the particular experimental details are recorded in Table 3.1 and the aspect of the irradiated area is presented in Fig. 3.1.1.

The effects of these laser treatments were examined using confocal microscopy. Particular attention has been given to the border of the treated area in order to have better comparisons between radiated and original surface and because in these regions the effect of the laser is stronger as we have explained in section 2.2.1.

With some of the conditions at the higher fluence values, Fig. 3.1.2 shows that several cracks are generated in the glass, always in the perpendicular direction in comparisons to the scanning one. In particular, this is observed when the fluence reaches values higher than 2.79 J/cm^2. Fig. 3.1.3 shows an example of the measurement of the topography in these regions.

Fig. 3.1.1 Photograph of the bottle after laser treatment

Table 3.1 Parameters used in the laser treatments performed on irradiation regions

Irradiation regions	1	2	3	4	5	6
Pumping power (A)	5.00	5.30	5.60	6.00	6.30	6.60
Laser power (W)	1.00	1.12	1.25	1.40	1.57	1.70
Spot fluence (J/cm^2)	1.47	1.64	1.84	2.06	2.31	2.50
Spot irradiance (MW/cm^2)	4895.19	5482.61	6118.99	6853.27	7685.45	8321.83
Irradiation regions	7	8	9	10	11	
Pumping power (A)	7.00	7.15	7.25	7.50	8.00	
Laser power (W)	1.90	1.975	2.025	2.15	2.40	
Spot fluence (J/cm^2)	2.79	2.90	2.97	3.16	3.52	
Spot irradiance (MW/cm^2)	9300.86	9668.00	9912.76	10524.66	11748.46	

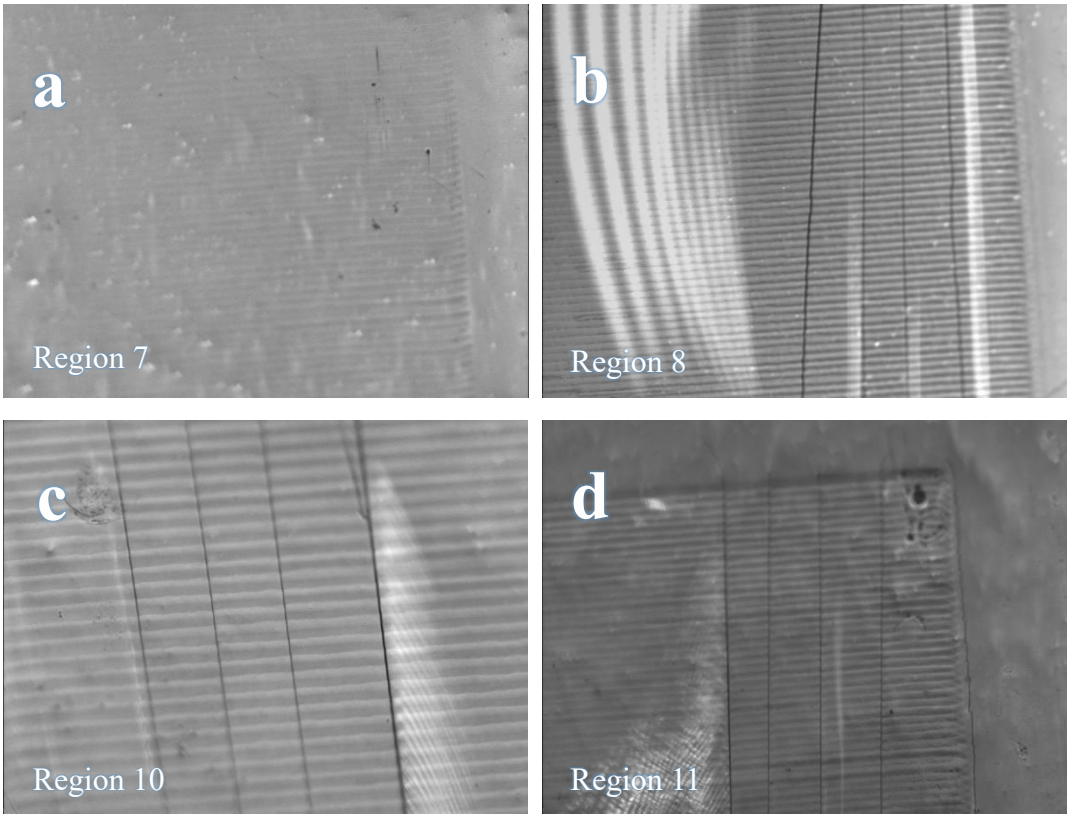

Fig. 3.1.2 Images obtained with confocal microscope of irradiation regions 7(a), 8(b), 10(c) and 11(d) on the borders between treated and untreated areas

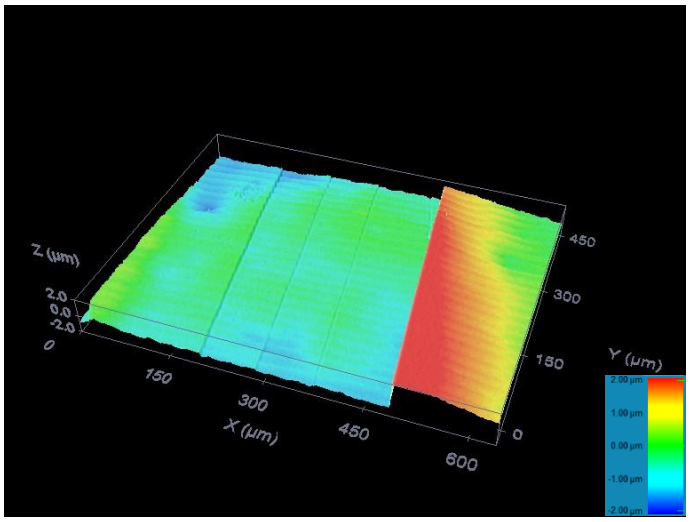

Fig. 3.1.3 Image obtained with confocal microscope of irradiation region 10 showing the defects that are generated in the glass topography

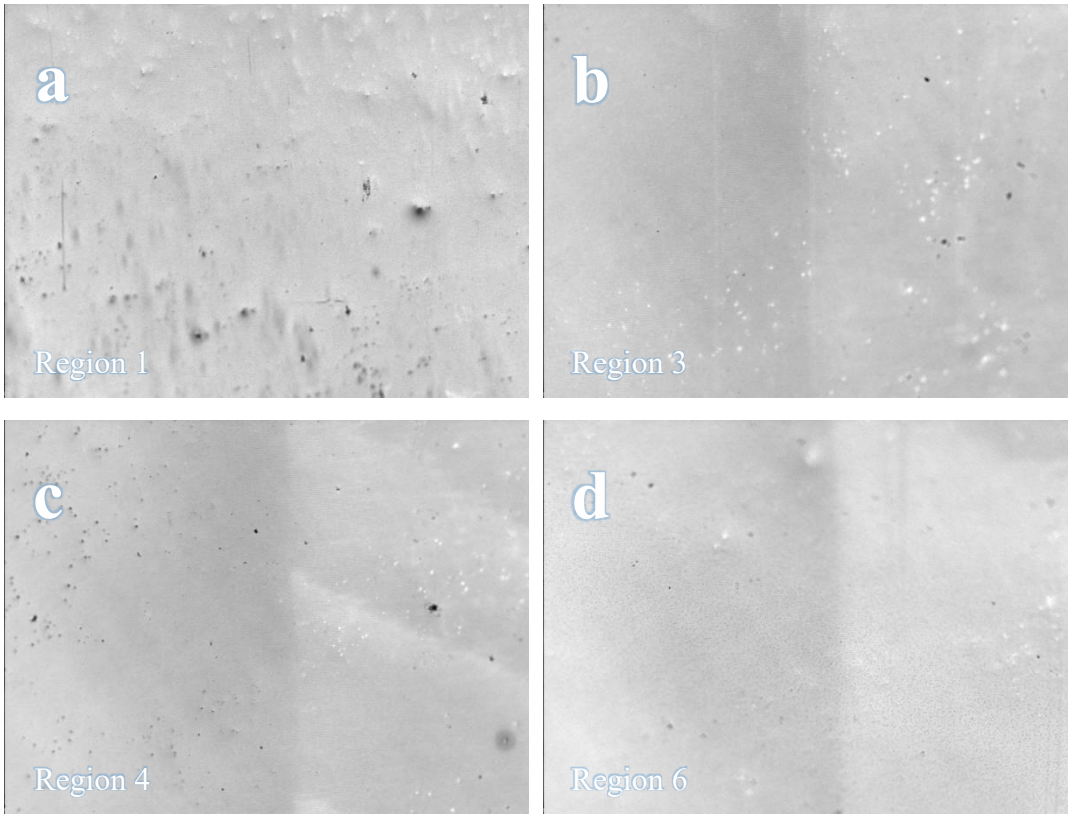

Fig. 3.1.4 Images obtained with confocal microscope of irradiation regions 1(a), 3(b), 4(c) and 6(d) on the borders between treated and untreated areas

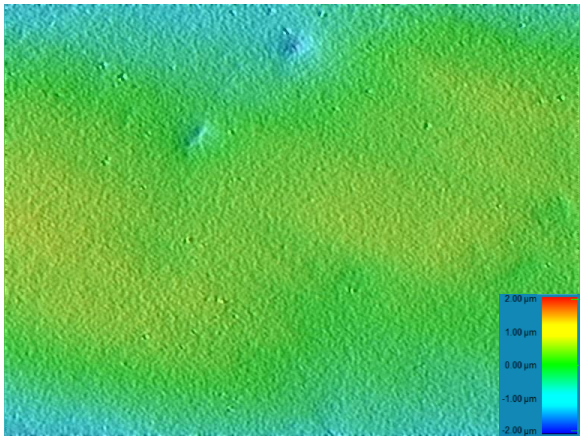

Fig. 3.1.5 Image obtained with confocal microscope of irradiation region 6 showing no change in the topography

Fig. 3.1.4 shows some examples of the regions treated with lower fluence values. With these laser conditions, only small relative changes in morphology were observed. No straps or cracks were generated on the surface of the treated areas. As it can be observed in Fig. 3.1.5, the confocal scans also do not show measurable changes in the surface topography. This indicates that no damage or removal of the

glass substance occurred below an energy density of 2.50 J/cm^2. The ablation threshold and alteration threshold for the brown industrial glass sample were determined by confocal microscopy regarding the impact of the laser treatment. The results show that the ablation threshold is between 2.50 J/cm^2 and 2.79 J/cm^2.

The alteration threshold is another important parameter that marks the energy density below which no recognizable impact of the laser beam could be observed (Fekrsanati et al., 2001). Following the results obtained in these experiments, this alteration threshold is below 1.47 J/cm^2.

3.2.- Effect of using the UV laser to process transparent industrial glass

A similar set of experiments has been performed in a transparent glass, using also a continuous bidirectional configuration, a frequency of 300 kHz, a scanning speed of 50 mm/s and a distance between scanning lines of 10 microns. In this case the spot fluence has been modified from 1.47 J/cm^2 up to 4.26 J/cm^2 (Table 3.2). As it can be observed in Fig. 3.2.1, glass has been painted with red ink in order to clearly identify where laser treatments have been performed and also to evaluate its cleaning capability.

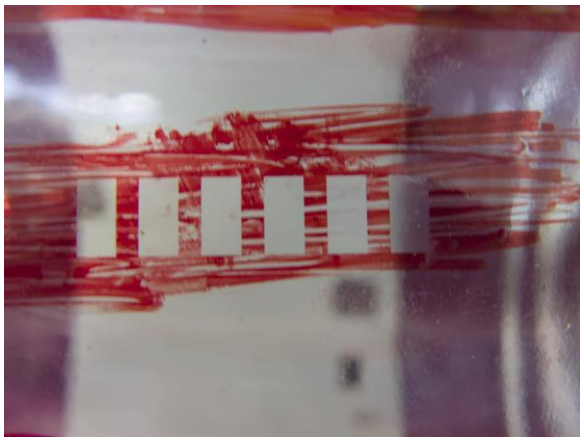

Fig. 3.2.1 Photograph of the transparent glass recipient after laser treatment

Table 3.2 Parameters used in the laser treatments performed on irradiation regions

Irradiation regions	1&2	3	4	5	6	7	8
Laser power (W)	1.00	1.90	1.975	2.025	2.15	2.40	2.90
Spot fluence (J/cm^2)	1.47	2.79	2.90	2.97	3.16	3.52	4.26
Spot irradiance (GW/cm^2)	4.9	9.3	9.7	9.9	10.5	11.7	14.2

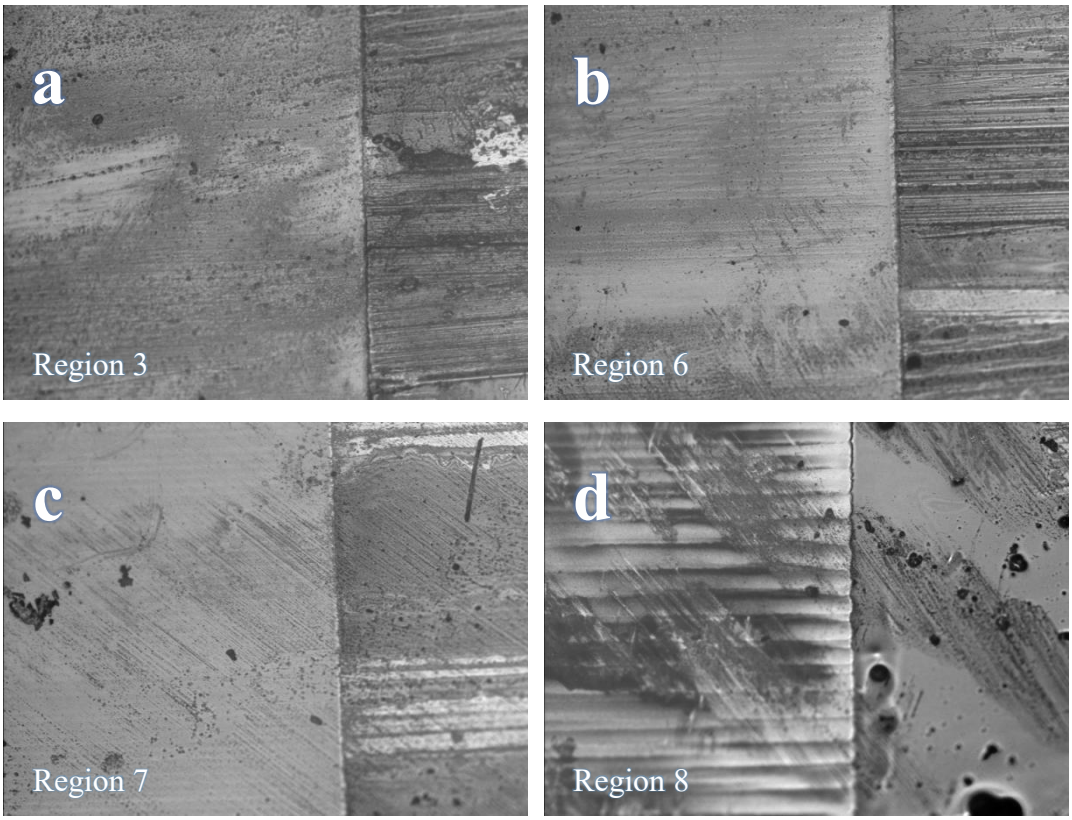

Fig. 3.2.2 Images obtained with confocal microscope of irradiation regions 3(a), 6(b), 7(c) and 8(d) on the borders between treated and untreated areas

The images of Fig. 3.2.2 and Fig. 3.2.3 show how the surface morphology and topography were altered during the laser treatment. There is a clear tendency to remove the red paint completely with increasing spot fluence from 2.79 J/cm^2 to 4.26 J/cm^2. High-fluence irradiations also induced high morphological alterations in the glass surface. Wide parallel stripes were observed in the laser irradiation region 8 when the spot fluence reached a value of 4.26 J/cm^2. The surface topography of this region, with a higher roughness, also showed the traces of the scanning direction,

which indicates that the ablation of the material has taken place during the laser treatment (see Fig. 3.2.3).

On the other hand, as shown in Fig. 3.2.4 and Fig. 3.2.5, no significant change in morphology and topography of the sample surface was observed at relatively low fluence of 1.47 J/cm^2. From these results, ablation threshold between 3.52 to 4.26 J/cm^2 and alteration threshold between 1.47 to 2.79 J/cm^2 for this transparent glass sample were determined. As it can be seen, both ablation threshold and alteration threshold of this sample are higher than those of the brown industrial glass sample.

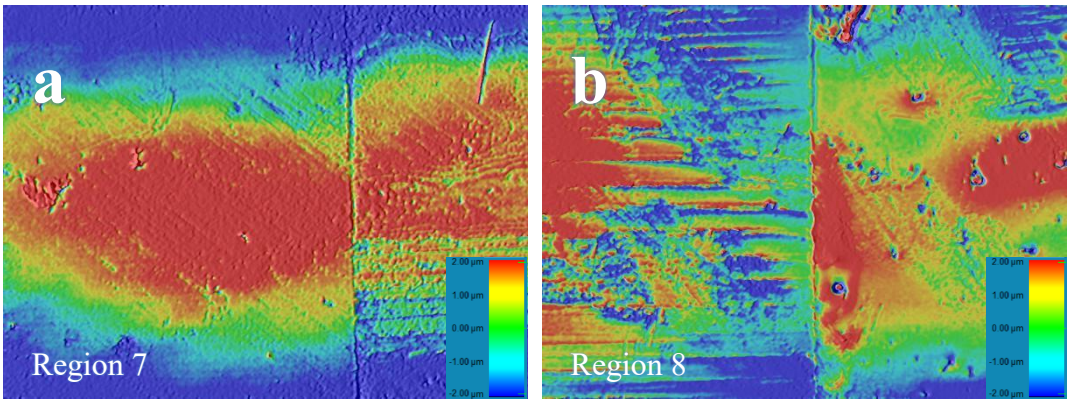

Fig. 3.2.3 Images obtained with confocal microscope of irradiation regions 7(a) and 8(b) showing changes in the topography

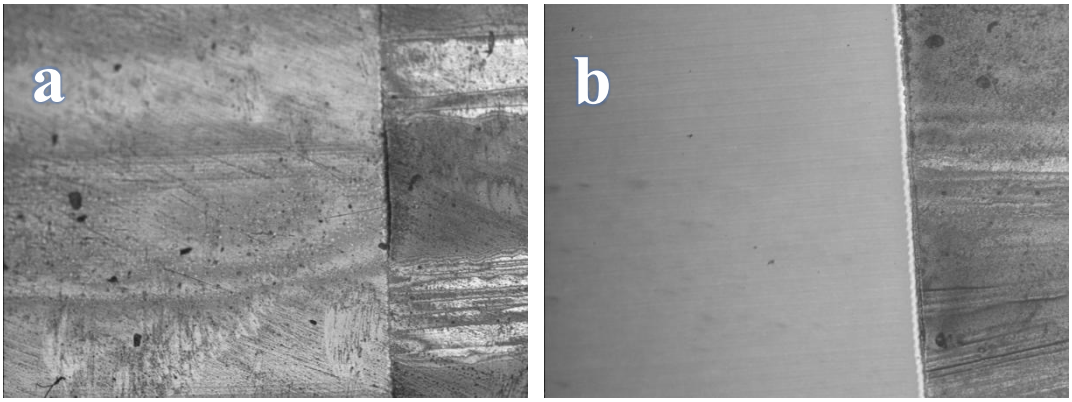

Fig. 3.2.4 Images obtained with confocal microscope of irradiated regions treated using the lowest fluence value with 1 pass (a) or 5 passes (b)

As it can be observed, when the lowest value of the fluence (1.47 J/cm^2) was used the glass was not damaged. Whit these conditions, the effect of multiple laser passes has been studied. As shown in Fig. 3.2.4(a) and Fig. 3.2.5(a), when the

sample was irradiated once the red paint was partially removed and the original surface was not damaged. But the treatment was not enough to remove all the red paint as some parts of the paint were still observed. In order to test the possibility for further removal of the red paint with these low spot fluence values, the laser treatment was repeated five times. The observation of the surface (Fig. 3.2.4(b) and Fig. 3.2.5(b)) reveals that it has been possible to remove completely the red paint and that the sample surface has not been damaged. The results show that multiple laser passes can improve the cleaning performance without inducing further alterations in glass substrate.

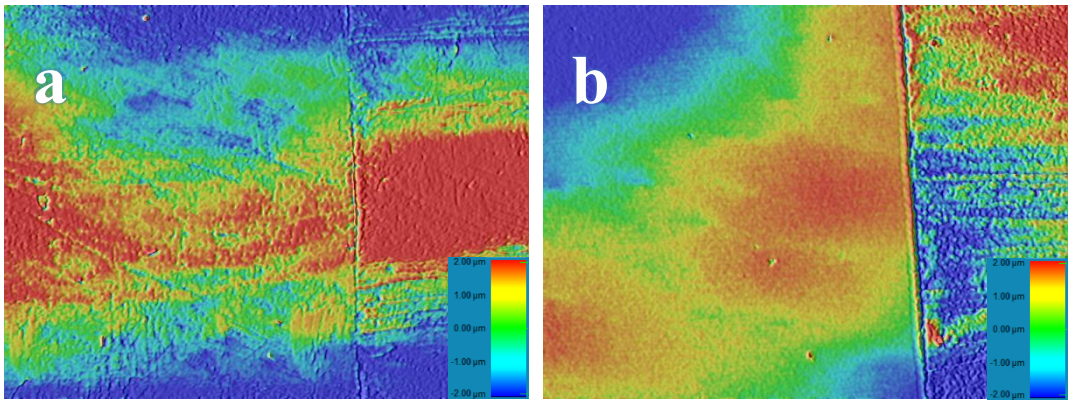

Fig. 3.2.5 Confocal images showing the topography of the two images presented in Fig. 3.2.4.

3.3.- Effect of using the n-IR laser to process industrial glass

Laser treatments have also been performed in the industrial glass using the n-IR laser. For making direct comparisons between the UV laser and the n-IR laser, almost the same parameters as reported earlier were used. It was found in the experiment that a lot of heat was generated on the surface of the brown industrial glass during the laser treatment. The sample cracked due to thermal stresses generated by laser induced local overheating, as shown in Fig. 3.3.1(a). The transparent industrial glass has a high transmittance to the n-IR laser beam. The laser can effectively remove the red paint while at the same time having no significant influence on the glass substrate even with a high applied energy (Fig. 3.3.1(b)). This is exactly what we need. Considering that the historical glass sample to be cleaned is transparent, n-IR laser was mainly used for the cleaning of the stained glass sample in the later

experiment.

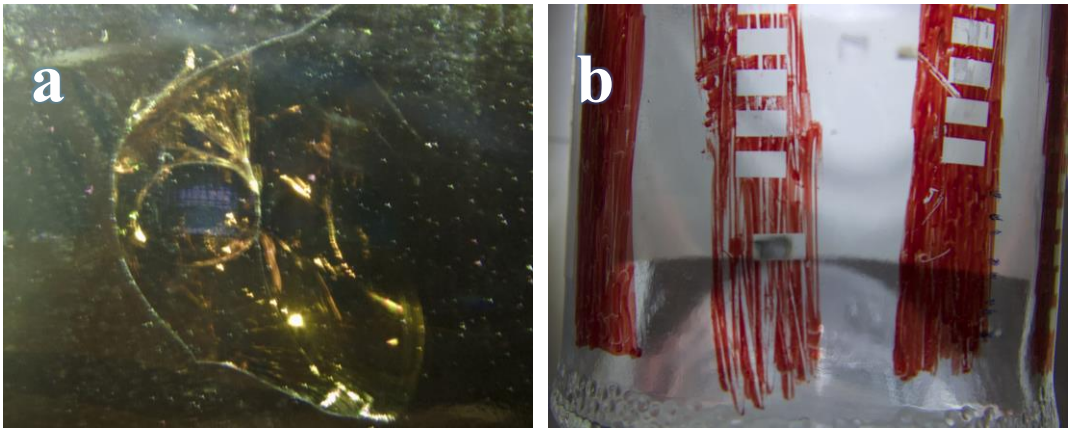

Fig. 3.3.1 Photographs of both industrial glass samples showing the effect of the n-IR laser

3.4.- Elimination of surface cracks in window glass

Laser technologies can also be used to treat regions with cracks on the surface. To do this, it is important to melt a thin layer on the surface of the glass in a controlled way. Usually, these melting treatments can be done using continuous CO_2 lasers. Obviously, in order to avoid crack formation the laser treatment has to be performed at high temperatures, of the order of 500ºC. This limits the possible application of this technology in some cases.

Fig. 3.4.1 shows an example of a window glass after been treated with a CO_2 laser. Surface of the sample was scratched before laser treatment. The figure clearly shows that the laser treatment has reduced considerably the depth of the scratches.

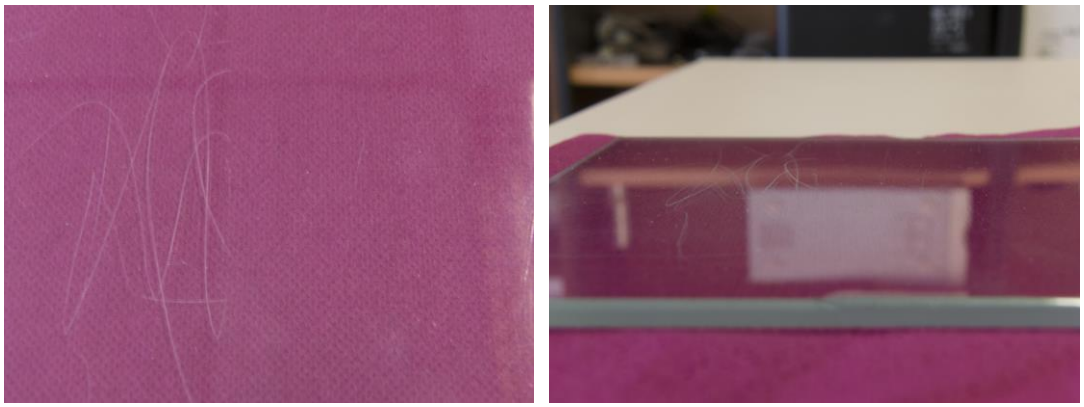

Fig. 3.4.1 Scratched window glass after being treated with a CO_2 laser

CHAPTER 4: DEVELOPING LASER PROCESSES TO TREAT LOCALISED AREAS

Usually, in Cultural Heritage, the areas that have to be cleaned do not have a uniform microstructure and to use a uniform laser-cleaning process could not be appropriate because it can be too strong for some areas and too soft for others. Taking into account this behavior, it is important to define a laser-cleaning protocol where the laser treatment can be adjusted in each region of the surface.

4.1.- Developing a system to define areas where laser treatment has to be performed

The protocol to define areas where leaser treatment has to be developed based on taking a photograph of the sample surface, to manipulate in order to define where the treatment has to be performed and to select the best laser configuration to treat it.

A color image of the sample is taken using a CASIO EX-FH20 digital camera. The camera was placed at a given position between the laser and the sample and then it was calibrated horizontally with a spirit level. The captured image was stored in RAW format to avoid loss of quality.

Once the image is stored, two ways to transform it have been evaluated. In the first one, modification of the image was performed by using a graphics editing software (Adobe Photoshop), which includes adjusting the grayscale shade and converting the image to black and white. The resulting image was then exported as a bitmap file. This file was imported into the motion control software (Visual Laser Marker) of the laser apparatus and then converted into the machine code that the system uses to define the location corresponding to each marking pixel. The black and white image in Fig. 4.1.1 shows an example of a bitmap pattern loaded onto the laser

system. It corresponds to the stained glass sample presented in Fig. 2.4.1. The black regions of the image correspond to the regions that we want to clean with the laser, while the white regions are associated to regions where additional laser treatment is not required. Obviously, this image processing only can be applied when the bitmap laser scanning mode is applied with all the limitation that have been indicated in section 2.2.3.

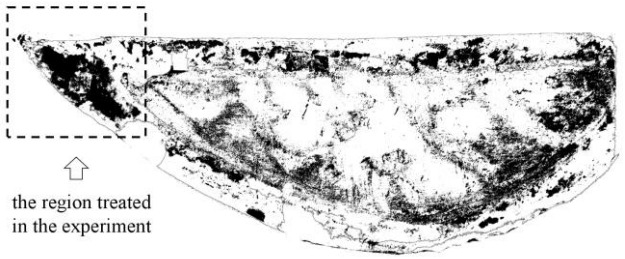

Fig. 4.1.1 Exemplary black and white image, which defines the bitmap scanning

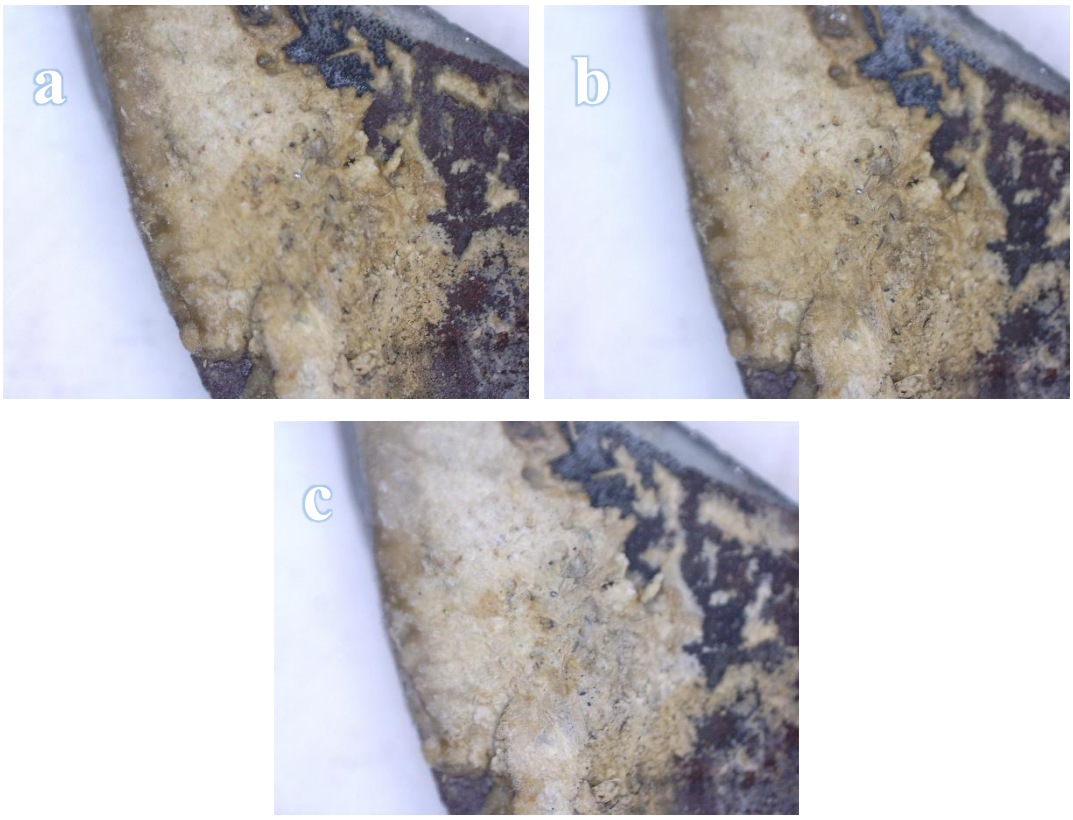

Fig. 4.1.2 Photographs of the transparent stained glass sample taken with optical microscope
(a) before treatment; (b) after IR laser irradiation;
(c) after both IR and UV laser irradiation

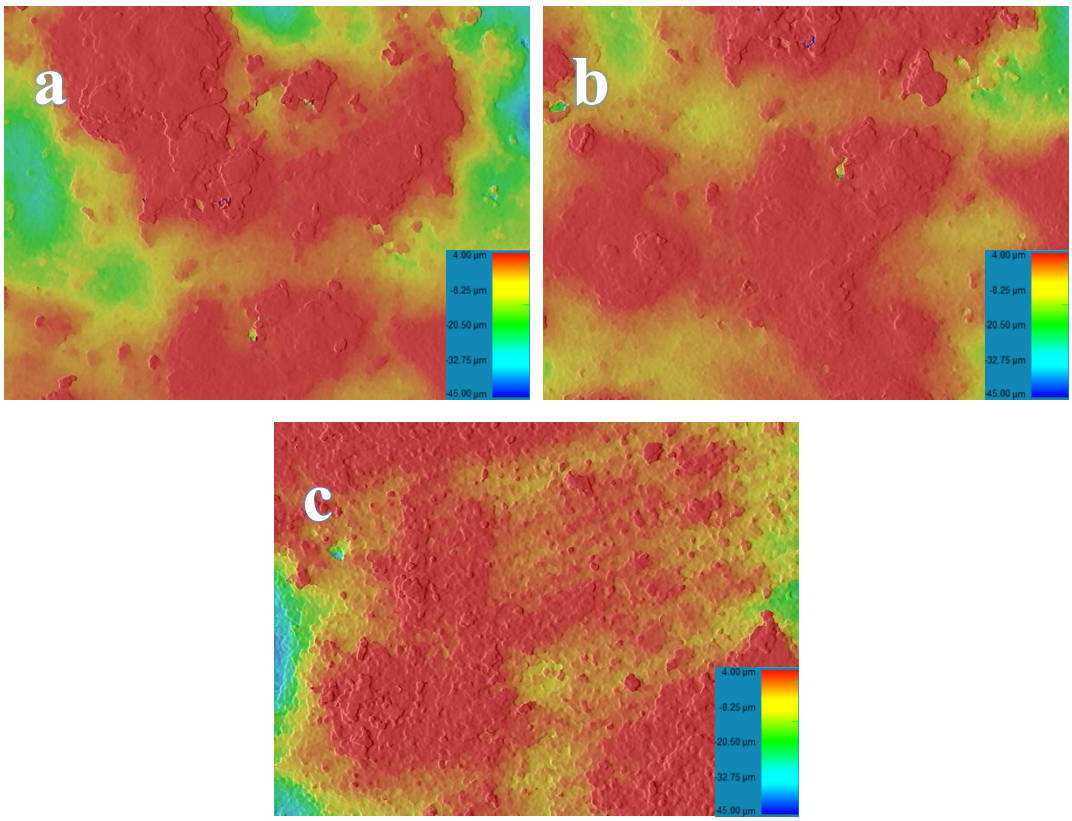

Fig. 4.1.3 Images obtained with confocal microscope showing the topography of the irradiation region. (a) before treatment; (b) after IR laser irradiation; (c) after both IR and UV laser irradiation

Using this configuration, a region of the sample (see Fig. 4.1.1) has been treated. The sample surface was scanned by the IR laser beam first and then scanned by the UV laser beam. Fig. 4.1.2 shows the photographs of the same region on the sample surface obtained with an optical microscope before and after the laser treatments. As the figure shows, the crust was almost unaffected by the IR laser treatment, then the UV laser caused minor changes in the microscopic surface morphology. Consistent with this, images obtained with confocal microscope from the same treated area (Fig. 4.1.3(a) and Fig. 4.1.3(b)) show no change in the surface topography before and after the IR laser treatment. The differences in surface topography between Fig. 4.1.3(b) and Fig. 4.1.3(c) can be explained by different reactions and/or absorbances of the crust with laser irradiation at different wavelengths, since it is accepted that IR laser pulses induce photothermal effects, while UV radiation produces photochemical effects (Pouli, 2000; Riveiro et al., 2018). As mentioned above, the laser parameters are not controlled with this

scanning mode. The only processing parameter that can be adjusted to control the process is the image resolution. However, it can be observed that both lasers were not sufficient to remove the crust using bitmap scanning mode, even at their maximum resolution.

The second alternative to process the image of the sample in order to define precisely the areas that need to be scanned is importing vector files created with graphics editing software (Adobe Photoshop and Adobe Illustrator) into the laser system control software (Visual Laser Marker). The process is similar to the steps taken when using the bitmap scanning mode. First a digital photograph was taken from the glass sample. Then, in Adobe Photoshop, the scanning areas were defined by selecting the pixels at the corresponding positions where the laser treatment was planned to be applied. The selection was turned into a work path and then exported to Adobe Illustrator, where the vector path was converted to the DXF format (Drawing Interchange Format) that can be imported into the Visual Laser Marker software. After the DXF file had been loaded, the position and scale of the loaded pattern were adjusted to ensure that the laser irradiation was performed within the boundaries defined previously.

The advantage of this processing protocol is that once the DXF file has been loaded, it is possible to define different laser parameters to each region, adjusting them to the characteristics of the area that has to be treated. In principle, when the continuous mode is used apart from the problems associated with the stop of the laser at the end of the lines, it has to be considered that these regions frequently have an irregular shape and the scanning line length changes while the scanning is performed. This can produce some inhomogeneities during the laser process.

For this reason, the analysis of the possibilities that this methodology opens has been performed using the burst mode. The flexibility of the burst mode, combined with the possibility for selective scanning provided by the laser system control software,

gives burst mode a significant advantage compared to bitmap mode, in which the only adjustable parameter is the image resolution; and also a more uniform energy distribution in comparison with the continuous mode.

We have prepared a laboratory glass where four regions have been painted with different colors (Fig. 4.1.4(a)). The objective was to eliminate the two regions that were painted in black. Fig. 4.1.4(b) shows the image of the sample after having defined the four regions and we selected the black regions in order to clean them.

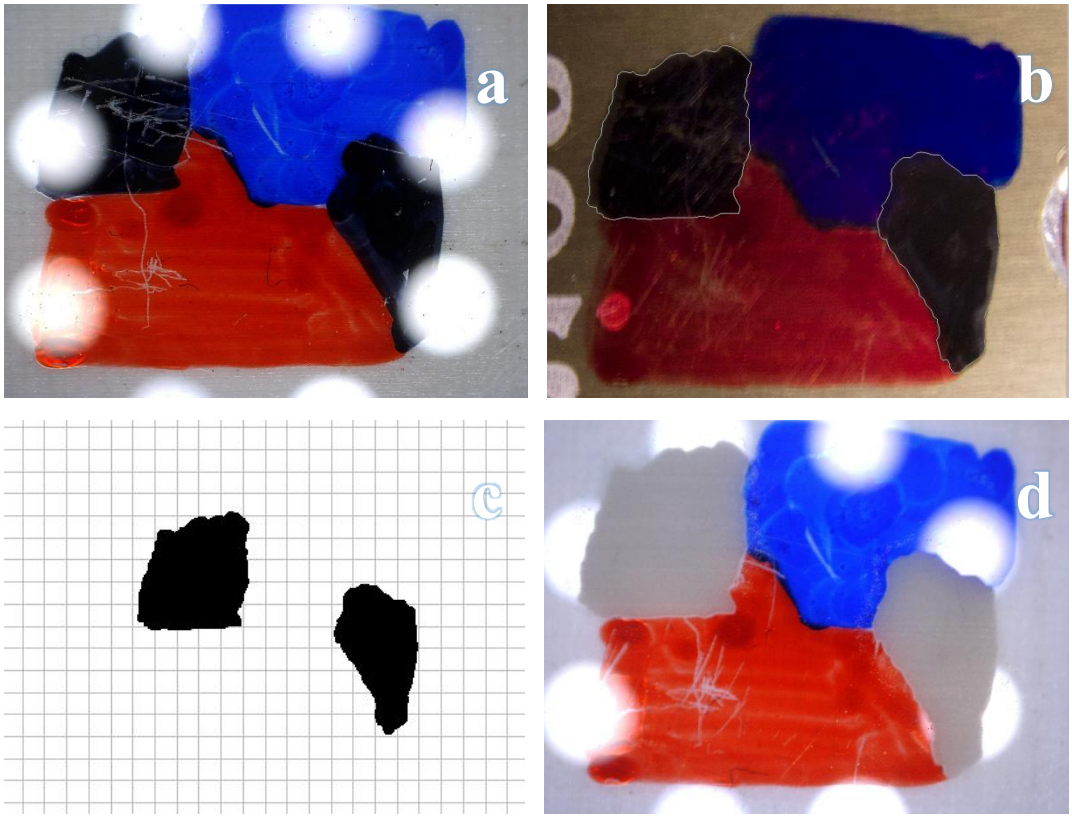

Fig. 4.1.4 Selective removal of black paint from glass.
(a) the glass sample before treatment; (b) digital image of the glass sample showing the selected areas; (c) the vector path (DXF file) imported into the laser system control software;
(d) the result of the selective laser treatment

The experiment was performed with the UV laser operating in the burst mode. The laser parameters that have been fixed are the frequency (300 kHz) and the power (2.90 W). Along the scanning direction the distance between pulses was selected to be 0.03 mm while the distance between scanning lines was 0.01 mm. In each point,

the number of pulses was fixed to 100. In consequence, in each point the energy of one pulse was 9.67 μJ, producing a total fluence of 426 J/cm^2.

The result of the experiment is shown in Fig. 4.1.4(d). A relatively satisfactory result could be observed. Areas irradiated with laser show that most of the black paint was successfully removed after the treatment. There remains little visible evidence of the black paint that had been originally applied to the glass surface because in the scanning direction the laser dots do not overlap. On the other hand, a spatial control of cleaning area with high precision was achieved. The laser radiation was tightly confined to the black areas, leaving the adjacent areas unaffected. The precise removal of black paint from the glass sample is a good example demonstrating the effectiveness and accuracy of the presented method for selective laser cleaning.

It has to be noted here that the aluminum foil under the glass was ablated during the laser treatment (Fig. 4.1.5). The particles ejected from the aluminum during ablation stuck to the bottom surface of the glass, generating a metallic coating in the glass surface that was in contact with the support. Special attention should be paid to avoid this kind of problem when cleaning at a relatively high fluence values, keeping always a space of at least 2 mm between the glass and the support.

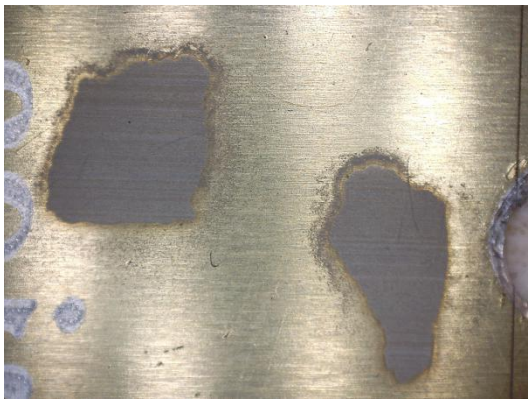

Fig. 4.1.5 Photograph of the aluminum foil under the glass after laser treatment

4.2.- Example with a stained glass sample

A small segment of continuous crust layer on the stained glass surface was selected to explore the applicability of the selective cleaning method described before. The experiment was performed with the n-IR laser operating in the burst mode. Selection of laser treatment parameters was based on previous experiment with samples of modern glass and pre-testing on inconspicuous areas of this stained glass sample. The number of pulses in a burst was 20 and the energy of every single pulse was about 8.27 μJ. Details on the laser and scanning parameters are provided in Table 4.1. The progress of laser treatment was assessed with optical microscopy and scanning electron microscopy by examining the sample after different number of laser passes. The results are shown in Fig. 4.2.1 and Fig. 4.2.2.

Optical and SEM micrographs show that with an increase in the number of laser passes, larger amounts of crust were ablated and melted. It can be observed in Fig. 4.2.1 that more areas of the crust layer exhibit a change in color from yellow to white. Correspondingly, in Fig. 4.2.2, these areas show a change in morphology from a compact and earthy-like microstructure to a loose and porous texture. An obvious side effect of laser cleaning observed in these images was the melting of the paint outside the desired cleaning area, which was caused by the misalignment of the laser beam (illustrated by arrows in Fig. 4.2.1(b)). This misalignment may be due to inaccuracy or errors introduced in the operation process.

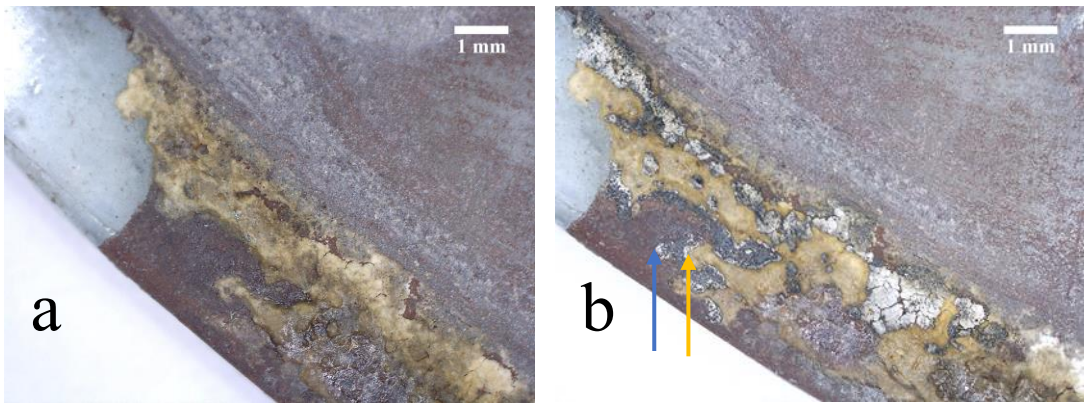

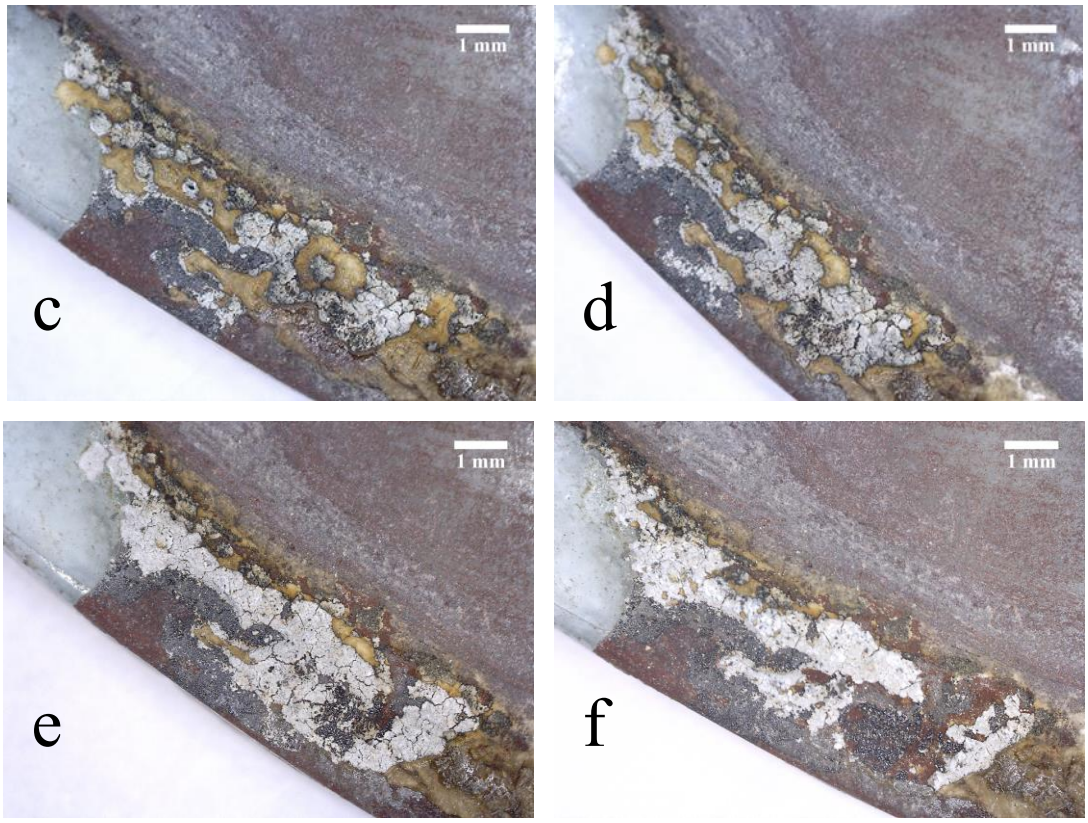

Fig. 4.2.1 Optical microscopic images showing the surface morphology of the sample after different number of laser passes
(a) before treatment; (b) 5 passes; (c) 10 passes; (d) 15 passes; (e) 30 passes; (f) 50 passes

Table 4.1 Parameters used in the selective laser cleaning performed on stained glass sample

Stained glass sample			
Pumping power (A)	4.00	Distance between scanning lines (mm)	0.015
Laser power (W)	2.48	Number of passes	50
Number of pulses in a burst	20	Spot fluence (J/cm^2)	33.68
Inter burst space (mm)	0.03	Spot irradiance (MW/cm^2)	0.505

In the end the laser cleaning resulted in the removal of a small part of the crust layer and a reduced thickness of the crust remained. However, most paint located close to or beneath the crust layer was melted, even though in a small area the paint seemed unaltered after the crust was removed (Fig. 4.2.1(f)). The total removal of

the crust layer can probably be achieved by increasing the applied power and the number of treatment times, which can also result in further damage to the delicate paint. It can be concluded that selective laser cleaning is a feasible technique for relatively precise and controllable cleaning of stained glass, but considering the limitation and side effect, caution must be taken in its application.

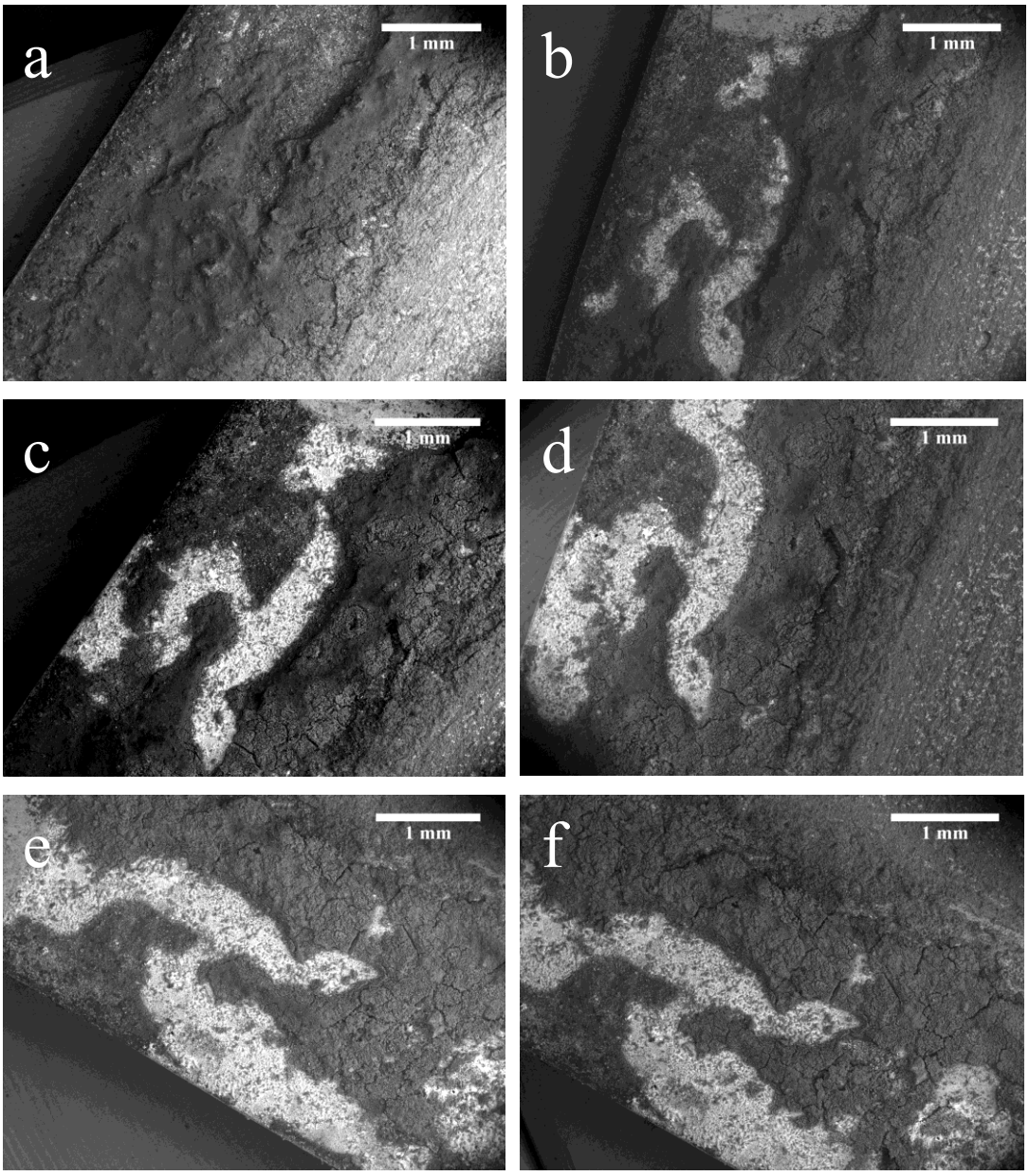

Fig. 4.2.2 SEM images showing the surface morphology of
the sample after different number of laser passes
(a) before treatment; (b) 5 passes; (c) 10 passes; (d) 15 passes; (e) 30 passes; (f) 50 passes

CHAPTER 5: CHARACTERIZATION OF THE MODIFICATIONS THAT LASER TREATMENTS INDUCE IN STAINED GLASS

The modifications that laser treatments induce in a stained glass sample have been analyzed using FESEM-EDS. As shown in Fig. 5.1.1, a small corner fragment was cut from the stained glass sample for this characterization with the UV laser in order to avoid the generation of cracks in the sample. Since the FESEM must be operated at a high level of vacuum, a carbon coating is necessary in the glass surface. This area has been selected because it is possible to remove the corner fragment without causing any visible effect on the window, as this location will be hidden under lead cames if the window is reinstalled. Fig. 5.1.2(a) shows the photograph of this corner fragment taken with optical microscope before treatment. It can be observed that most of its external surface was covered by a thick layer of yellowish crust and also that some previous laser treatments have been performed before this study in two regions of the sample (indicated with red circles in the Figure).

Fig. 5.1.1 A small corner fragment was cut from the stained glass sample

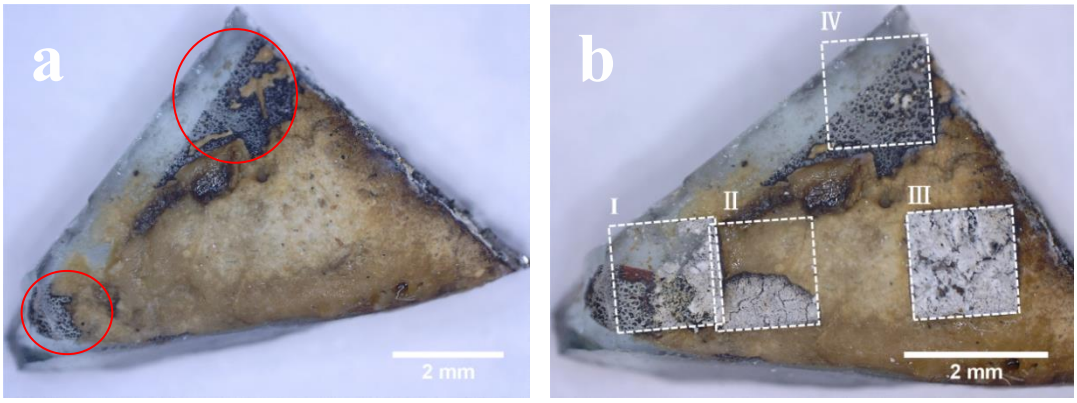

Fig. 5.1.2 Photographs of the corner fragment taken with optical microscope
(a) before treatment; (b) after treatment

The laser treatment was carried out using the IR laser in burst mode and 4 irradiation fields of 2.25 mm^2 (1.5mm × 1.5mm) were applied on the surface of the corner fragment where the crust is present. It is also important to take in mind that in this side of the glass is where paint is also present. The locations of the four regions are shown in Fig. 5.1.2(b), and the laser parameters used in each of the irradiation regions are described in Table 5.1. These conditions are the same in regions I, III and IV and smother in region II.

Table 5.1 Parameters used in the laser treatments performed on irradiation regions I-IV

Irradiation regions	I	II	III	IV
Pumping power (A)	5.00	4.00	5.00	5.00
Laser power (W)	3.4	2.48	3.4	3.4
Number of pulses in a burst	20	20	20	20
Inter burst space (mm)	0.02	0.02	0.02	0.02
Distance between scanning lines (mm)	0.02	0.02	0.02	0.02
Number of passes	30	30	30	30
Spot fluence (J/cm^2)	46.18	33.68	46.18	46.18
Spot irradiance (MW/cm^2)	0.692	0.505	0.692	0.692

The image taken with optical microscopy after laser treatment (Fig. 5.1.2(b)) shows that the surface morphology of all the irradiation regions has been altered. For region I, some thin crusts have been removed from the surface and a part of paint under the crust layer has been melted. The glass substrate was also affected in the area where the paint was melted. In addition, it can be clearly seen in the image that laser irradiation successfully removed the crust in a small area without affecting the paint beneath, which is the desirable result in accordance with the conservation principle. In the case of region II with a lower irradiance value, it can be seen that the morphology of the upper part of this region was little affected by laser radiation and remained nearly the same as before treatment. While the lower part of this region was strongly affected by laser treatment, resulting in a change in color from yellowish to white. The high irradiance in region III led to a change in color within the whole region, whereas the removal effect was relatively limited even if the laser treatment was repeated 30 times. It was observed in the experiment that the removal effect was weaker with an increase in the number of laser passes. Presumably this was due to the decrease of absorbance at 1064 nm, which was caused by the change in color of the crust during the treatment. For region IV, some of the deposits were removed from the surface, and no visible effect on the glass substrate (upper left part of the region) can be observed.

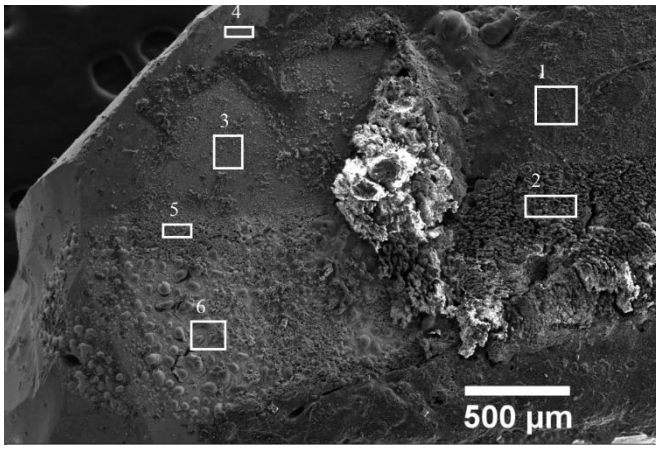

Fig. 5.1.3 Image taken with FESEM of the irradiation regions I and II

Table 5.2 Results of EDS analysis for irradiation regions I and II (at%)

Zone	O	Na	Mg	Al	Si	P	S	Cl	K	Ca	Fe	Cu	Pb
1	70.48	1.10	11.01	0.69	1.84	/	0.30	0.52	0.41	13.25	/	/	0.39
2	52.20	/	13.47	0.80	2.03	/	/	/	0.38	31.12	/	/	/
3	57.95	3.58	4.13	1.81	18.86	0.54	/	/	2.84	7.37	0.42	/	2.48
4	54.10	4.88	2.50	2.06	24.24	0.40	/	/	3.74	5.09	0.34	0.23	2.43
5	59.60	1.32	4.41	1.15	6.81	/	/	0.34	1.00	6.16	16.6	/	2.61
6	56.20	2.73	2.78	1.29	10.98	/	/	/	1.71	5.54	11.78	/	6.99

Fig. 5.1.3 shows the location of the zones analyzed with EDS. Higher magnification images of each zone are shown in Fig. 5.1.4. Zone 1 corresponds to an area of the crust that was little affected by laser treatment. FESEM examination of this area showed an earthy and compact microstructure, as displayed in Fig. 5.1.4(a). While zone 2 corresponds to the crust that was strongly affected by laser radiation. FESEM image of this area (Fig. 5.1.4(b)) shows a relatively porous texture, and some melting can be observed. EDS results (Table 5.2) show that the amount of oxygen, calcium and magnesium in the crust is fairly high in comparison to the amount of other elements (data is presented in atomic percentage). The crust could be attributed to residual deposits of putty and/or cementing materials used to fix glass pieces into lead cames, since putty was commonly composed of calcium and/or magnesium carbonates mixed with linseed oil or other organic compounds as binding media (García-Heras et al., 2005). When comparing EDS results between these two zones, it can be clearly observed that the average amount of oxygen detected in zone 2 is significantly lower than the amount detected in zone 1. Correspondingly, the relative content of calcium is higher in zone 2 compared with zone 1. This may be due to the decomposition of calcium carbonate at high temperature, which released carbon dioxide during the process. Also, in the

original material the ratio Mg/Ca was 0.83 and was reduced to 0.43 after laser irradiation, indicting the ablation of Mg compounds.

Zone 3 corresponds to an area of the glass substrate that was irradiated by laser light, while zone 4 corresponds to a glass substrate region outside the irradiation regions. The FESEM image of zone 3 (Fig. 5.1.4(c)) shows that some deposits remained on the glass surface after laser treatment, and no noticeable alteration of the glass substrate can be observed. EDS results clearly show the composition of the glass (zone 4). As expected, the main component is SiO_2, with addition of NaO and CaO, as well as, and low impurities of other elements. In zone 3, the amount of Ca and Mg increases indicating that the particulates that are observed on the glass (Fig. 5.1.4(c)) correspond to the original crust (see Table 5.3).

Zone 5 corresponds to the paint layer that was little affected by laser irradiation. FESEM observation in this area (Fig. 5.1.4(e)) showed a porous and relatively homogeneous microstructure, which is in strong contrast to the paint in zone 6 (Fig. 5.1.4(f)). EDS results show that these two zones have a higher amount of iron comparing to other zones, which can be considered as the contribution of the chromophore oxides that give color to the paint. The crust that was originally in existence in these zones was removed by laser irradiation. Therefore, the amounts of calcium and magnesium in both zones are in the low ranges. In zone 6 the paint was melted, and its morphology changed to isolative protruding islands with irregular shape and size. EDS data confirmed the presence of high percentage of iron and silicon oxides, together with other elements. The amount of silicon in the protruding island formed by melted paint is relatively high. This result would strongly suggest the possibility of formation of a compound containing iron and silicon under the action of laser radiation, probably iron silicate. The high amount of silicon in the compound had most likely come from the glass substrate, creating some local defects on the glass surface (Fig. 5.1.5). In the regions between these islands, the amount of lead oxide strongly increases. Micro-cracks on the glass

surface can also be clearly observed in this zone. In the border of the region, a new phase, like a sponge, is observed. Its composition is very close to the original crust.

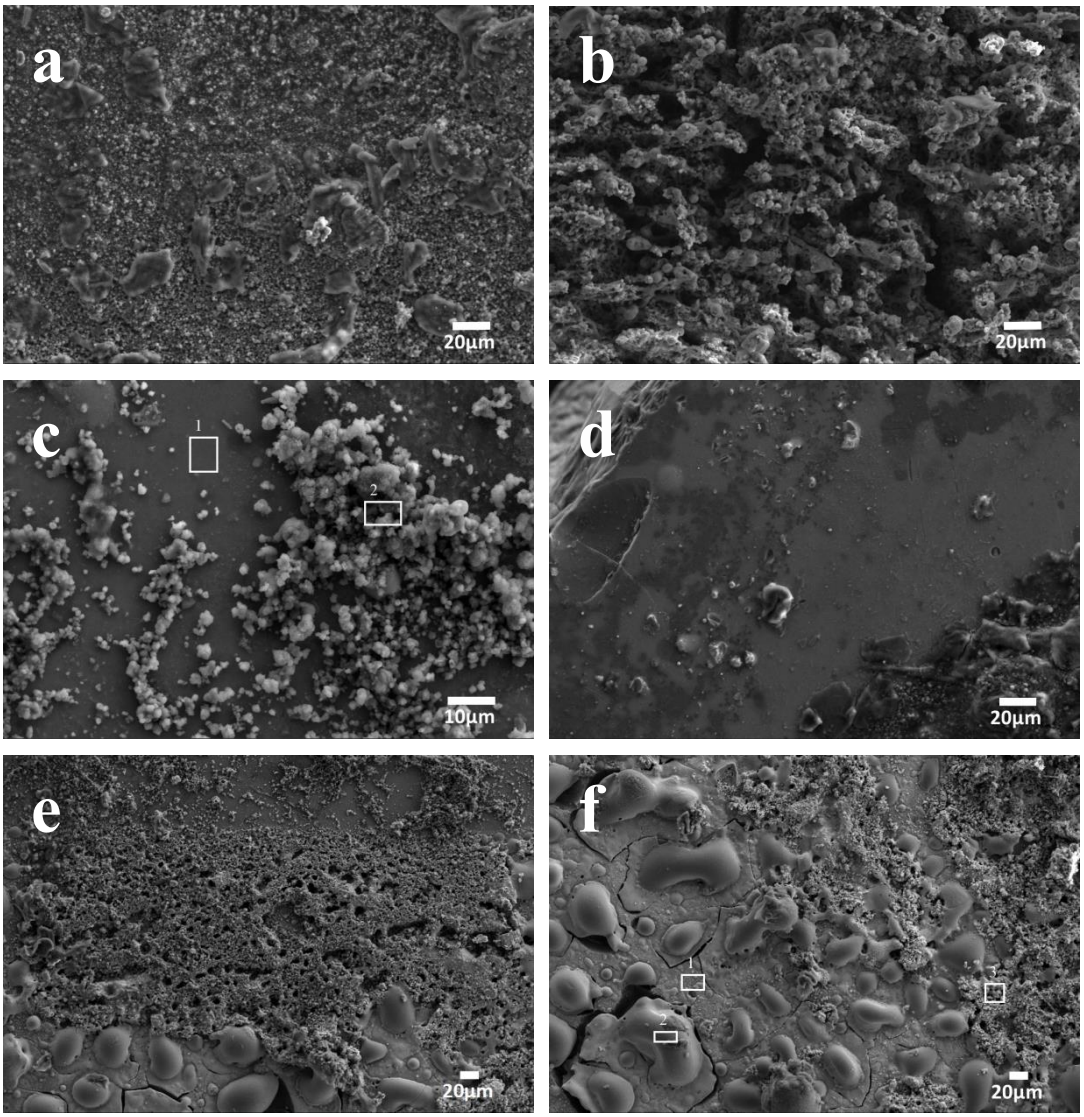

Fig. 5.1.4 Higher magnification FESEM images of each zone presented in Fig. 5.1.3
(a) zone 1; (b) zone 2; (c) zone 3; (d) zone 4; (e) zone 5; (f) zone 6

Table 5.3 Results of EDS analysis for irradiation region I zone 3 (at%)

Subzone	O	Na	Mg	Al	Si	K	Ca	Fe	Pb
1	55.40	4.26	2.50	2.07	24.25	3.72	4.96	0.32	2.51
2	65.32	0.31	13.36	2.41	2.76	0.15	15.25	/	0.44

Table 5.4 Results of EDS analysis for irradiation region I zone 6 (at%)

Subzone	O	Na	Mg	Al	Si	K	Ca	Fe	Pb
1	50.57	4.18	2.03	2.39	16.93	3.66	5.74	2.91	11.59
2	56.93	3.20	1.22	1.57	15.68	0.91	3.34	16.99	0.14
3	48.77	1.38	7.68	0.68	3.74	0.94	9.92	20.03	6.86

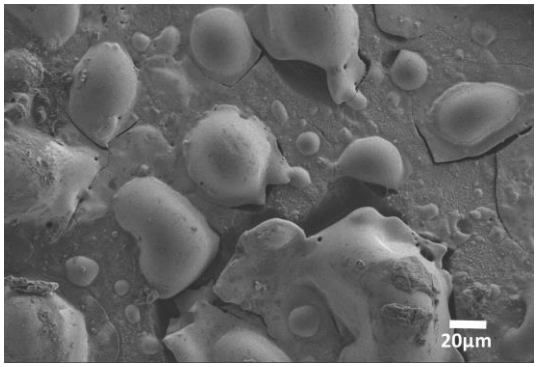

Fig. 5.1.5 Images taken with FESEM of the irradiation region I zone 6 showing the defects created on the glass surface

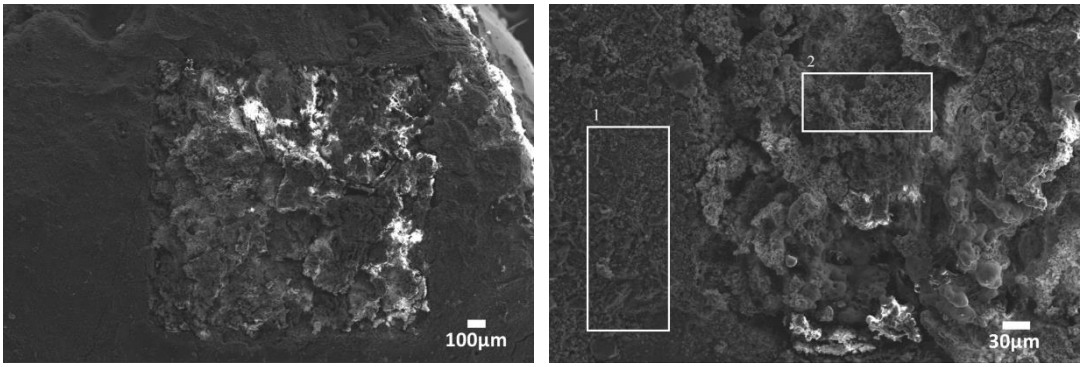

Fig. 5.1.6 Images taken with FESEM of the irradiation region III

Table 5.5 Results of EDS analysis for irradiation region III (at%)

Zone	O	Na	Mg	Al	Si	S	Cl	K	Ca	Pb
1	69.51	0.92	10.22	0.35	1.15	0.46	0.65	0.49	15.81	0.44
2	54.70	/	15.80	0.38	0.93	0.28	/	/	27.92	/

Fig. 5.1.6 shows FESEM micrographs of region III. The difference in the morphology between the non-treated (zone 1) and the treated region (zone 2) can be clearly seen. EDS data (Table 5.5) shows a similar evolution to that observed in zones 1 and 2 of region II. After laser irradiation oxygen content decreases and also the ratio Mg/Ca.

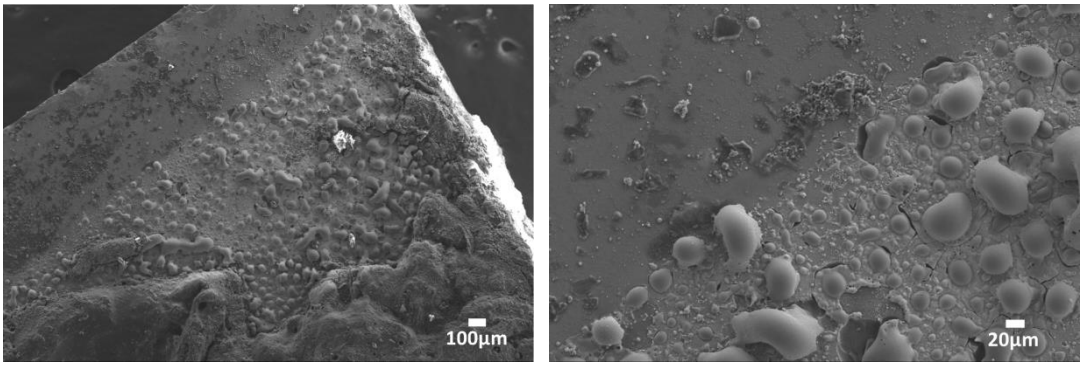

Fig. 5.1.7 Images taken with FESEM of the irradiation region IV

Finally, the detail of the microstructure in region IV clearly shows that when the laser acts directly on the glass, the sample is not damaged. By contrast, when the laser acts on the paint, it is melted, creating islands that are rich in Si and Fe, deteriorating the surface of the glass.

CONCLUSIONS

Stained glass windows are composed of shaped pieces of colored glass, held together in a lead metal network and enhanced with the surface application of a painted pigment. All the three elements are susceptible to deterioration. In the last two decades, some studies concerning laser cleaning of stained glass windows have presented promising results. In this work, an attempt is made to go a step further in the application of laser technologies in the restoration of stained glass. Several experiments have been conducted to investigate the interaction of laser radiation of different sub-nanosecond pulsed lasers (a UV laser and a n-IR laser) with different glass samples (a 16^{th} century stained glass sample and some commercial modern glass samples). The studies included in this thesis are summarized as follows:

The work has started by investigating the influence of different laser parameters in the cleaning process of commercial modern glass samples. First, effects of using the UV laser to process some commercial modern pieces of transparent and colored glasses were investigated. The ablation threshold and alteration threshold for these glass samples were determined by confocal microscopy regarding the impact of the laser treatment. The results show that the ablation threshold for the brown industrial glass is between 2.50 J/cm^2 and 2.79 J/cm^2, and the alteration threshold is below 1.47 J/cm^2. A similar set of experiments has been performed in the transparent industrial glass and the results showed that both ablation threshold and alteration threshold of this sample are higher than those of the brown industrial glass sample because the laser absorption is lower in this material. The possibility for improving the cleaning result by repeating the laser treatment was also tested on this sample. The results show that multiple laser passes can improve the cleaning performance without inducing further alterations in glass substrate. Laser treatment performed in the industrial glass using the n-IR laser showed that the laser damaged the brown industrial glass due to thermal stresses, but had no significant influence on the transparent colorless glass, even with a high applied energy.

One of the main contributions of this work has been to design a protocol to define areas where laser treatment has to be performed and even to have the possibility of using different laser parameters for each region. The method was based on taking a photograph of the sample surface, to manipulate it in order to define where the treatment has to be performed and to select the best laser configuration to treat it. Two different ways to transform the photograph have been evaluated. In the first one, the photograph was converted to a black and white bitmap image and the laser processing was carried out in bitmap scanning mode. The results showed that both UV and IR lasers were not sufficient to remove the crust from the stained glass using bitmap scanning mode because the possibilities that offer the laser control are very limited. The second alternative to process the image was to turn the selected area into a vector path and then import the file into the laser system control software. The areas that need to be scanned could be precisely defined transforming the image into a vector file, and it is also possible to define different laser parameters for each region, adjusting them to the characteristics of the area that has to be treated. Selective cleaning based on this approach was carried out on a prepared laboratory glass and a relatively satisfactory result was observed.

Furthermore, a small segment of continuous crust layer on the stained glass sample was selected to explore the applicability of this method. The experiment was performed with the n-IR laser operating in the burst mode because this laser does not affect the glass. Optical and SEM micrographs show the removal of a small part of the crust layer and a reduced thickness of the crust remained. But a misalignment was observed and some paint outside the desired cleaning area was melted. It was concluded that selective laser cleaning is a feasible technique for relatively precise and controllable cleaning of stained glass, but caution must be taken in its application.

A small corner fragment was cut from the stained glass for the characterization of the modifications induced by laser treatment. The surface morphology and chemical

composition of the sample were characterized by optical microscopy and FESEM-EDS. The results show that the glass substrate is mainly composed of SiO_2, with addition of NaO and CaO, as well as low impurities of other elements. The crust on the glass surface contains a high amount of calcium and magnesium carbonates, which could be attributed to residual deposits of putty. The amount of oxygen in the crust affected by laser radiation was reduced compared with the original material, which may be due to the decomposition of calcium carbonate at high temperature. The morphology of the paint was changed from a porous and homogeneous microstructure to isolated protruding islands with irregular shape and size when it was melted. The high amount of iron and silicon in the protruding islands suggests the possibility of formation of a compound containing these two elements, probably iron silicate. The high amount of silicon comes from the glass substrate, creating some local defects on the glass surface. Finally, it was confirmed that under the irradiation conditions of the present experiment, the stained glass sample was not damaged when the laser acted directly on the glass. In contrast, when the paint on the glass surface was irradiated by the laser, it melted and yielded islands that were rich in Si and Fe, resulting in a deteriorated glass surface.

REFERENCES

Arnold, H., 2014, Stained Glass of the Middle Ages in England and France, BookRix.

Asmus, J. F., 2003, LACONA: past, present, and future?, *Journal of Cultural Heritage*, **4**, 3-7.

Asmus, J. F., C. G. Murphy, and W. H. Munk, 1973, Studies On The Interaction Of Laser Radiation With Art Artifacts: Proc. SPIE 0041, Developments in Laser Technology II, p. 19-27.

Attard-Montalto, N., and A. Shortland, 2015, 17th century blue enamel on window glass from the cathedral of Christ Church, Oxford: Investigating its deterioration mechanism, *Journal of Cultural Heritage*, **16**(**3**), 365-371.

Basso, E., M. P. Riccardi, B. Messiga, M. Mendera, D. Gimeno, M. Garcia-Valles, J. Fernandez-Turiel, F. Bazzocchi, M. Aulinas, and C. Tarozzi, 2009, Composition of the base glass used to realize the stained glass windows by Duccio di Buoninsegna (Siena Cathedral, 1288–1289 AD): A geochemical approach, *Materials Characterization*, **60**(**12**), 1545-1554.

Becherini, F., A. Bernardi, A. Daneo, F. G. Bianchini, C. Nicola, and M. Verità, 2008, Thermal stress as a possible cause of paintwork loss in medieval stained glass windows, *Studies in Conservation*, **53**(**4**), 238-251.

Benton, J. R., 2009, Materials, methods, and masterpieces of medieval art, ABC-CLIO.

Bernardi, A., F. Becherini, G. Bassato, and M. Bellio, 2006, Condensation on ancient stained glass windows and efficiency of protective glazing systems: two French case studies, Sainte-Chapelle (Paris) and Saint-Urbain Basilica (Troyes), *Journal of Cultural Heritage*, **7**(**1**), 71-78.

Brown, S., and S. Strobl, 2002, A Fragile Inheritance: The Care of Stained Glass and Historic Glazing: a Handbook for Custodians, Church House Publishing.

Campbell, G., 2006, The Grove Encyclopedia of Decorative Arts: Two-volume Set, Oxford University Press.

Carmona, N., M. Villegas, and J. F. Navarro, 2006, Study of glasses with grisailles from historic stained glass windows of the cathedral of Leon (Spain), *Applied surface science*, **252**(**16**), 5936-5945.

Carmona, N., K. Wittstadt, and H. Römich, 2009, Consolidation of paint on stained glass windows: Comparative study and new approaches, *Journal of Cultural Heritage*, **10**(**3**), 403-409.

Carroll, J., R. Bradley, and A. Kalmikoff, 1994, Using waxes and polymers to improve coatings properties, *Surface coatings international*, **77**(**10**), 435-441.

Charleston, R. J., 1960, Lead in glass, *Archaeometry*, **3**(**1**), 1-4.

Cooper, M., and J. Larson, 1996, The use of laser cleaning to preserve patina on marble sculpture, *The Conservator*, **20**(**1**), 28-36.

Cooper, M. I., 1994, Laser cleaning of stone sculpture: Doctoral thesis, Loughborough University, Loughborough.

Cooper, M. I., D. C. Emmony, and J. Larson, 1995, Characterization of laser cleaning of limestone, *Optics & Laser Technology*, **27**(**1**), 69-73.

Delgado, J. M. L., 2016, Restoring medieval stained-glass transparency: use of new task specific luminescent ionic liquids for corrosion crusts removal: Master's thesis, Universidade Nova de Lisboa, Lisbon.

Drewello, R., and R. Weissmann, 1997, Microbially influenced corrosion of glass, *Applied Microbiology and Biotechnology*, **47**(**4**), 337-346.

Fekrsanati, F., S. Klein, J. Hildenhagen, K. Dickmann, Y. Marakis, A. Manousaki, and V. Zafiropulos, 2001, Investigations regarding the behaviour of historic glass and its surface layers towards different wavelengths applied for laser cleaning, *Journal of Cultural Heritage*, **2**(**4**), 253-258.

Fernandes, P., M. Vilarigues, L. C. Alves, and R. C. da Silva, 2008, Stained glasses from Monastery of Batalha: Non-destructive characterisation of glasses and glass paintings, *Journal of Cultural Heritage*, **9**, e5-e9.

Findakly, T., 1985, Glass waveguides by ion exchange: a review, *Optical engineering*, **24**(**2**), 242-244.

Fotakis, C., D. Anglos, V. Zafiropulos, S. Georgiou, and V. Tornari, 2006, Lasers in the preservation of cultural heritage: principles and applications, CRC Press.

García-Heras, M., N. Carmona, C. Gil, and M. A. Villegas, 2005, Neorenaissance/Neobaroque stained glass windows from Madrid: a characterisation study on some panels signed by the Maumejean Fréres company, *Journal of Cultural Heritage*, **6**(**2**), 91-98.

Godoi, R. H. M., V. Kontozova, and R. Van Grieken, 2006, The shielding effect of the protective glazing of historical stained glass windows from an atmospheric chemistry perspective: case study Sainte Chapelle, Paris, *Atmospheric Environment*, **40**(**7**), 1255-1265.

Hall, S., 2007, The Color of Light: Commissioning Stained Glass for a Church, Liturgy Training Publications.

Hrnjić, M., 2015, Application of Lasers for Surface Cleaning of Cultural Heritage Metals: Master's thesis, University of Évora, Évora.

Hu, W., Y. C. Shin, and G. King, 2010, Modeling of multi-burst mode pico-second laser ablation for improved material removal rate, *Applied Physics A*, **98**(**2**), 407.

Jembrih-Simbürger, D., C. Neelmeijer, O. Schalm, P. Fredrickx, M. Schreiner, K. De Vis, M. Mäder, D. Schryvers, and J. Caen, 2002, The colour of silver stained glass—analytical investigations carried out with XRF, SEM/EDX, TEM, and IBA, *Journal of Analytical Atomic Spectrometry*, **17**(**4**), 321-328.

Jenness, N. J., K. D. Wulff, M. S. Johannes, M. J. Padgett, D. G. Cole, and R. L. Clark, 2008, Three-dimensional parallel holographic micropatterning using a spatial light modulator, *Optics express*, **16**(**20**), 15942-15948.

Jones, T. W., and L. Matthews-Jones, 2016, Material Religion in Modern Britain: The Spirit of Things, Springer.

Kerse, C., H. Kalaycıoğlu, P. Elahi, B. Çetin, D. K. Kesim, Ö. Akçaalan, S. Yavaş, M. D. Aşık, B. Öktem, and H. Hoogland, 2016, Ablation-cooled material removal with ultrafast bursts of pulses, *Nature*, **537**(**7618**), 84-88.

Kibler, W. W., and G. A. Zinn, 2017, Routledge Revivals: Medieval France (1995): An Encyclopedia, Routledge.

Kleiner Fred, S., 2014, Gardner's Art through the Ages: A Global History, Cengate Learning.

Koh, Y. S., 2005, Laser cleaning as a conservation technique for corroded metal artifacts: Doctoral thesis, Luleå University of Technology, Luleå.

Krumbein, W. E., C. E. Urzì, and C. Gehrmann, 1991, Biocorrosion and biodeterioration of antique and medieval glass, *Geomicrobiology Journal*, **9**(**2-3**), 139-160.

Mahamood, R., 2018, Laser Basics and Laser Material Interactions, in *Laser Metal Deposition Process of Metals, Alloys, and Composite Materials*, 11-35, Springer.

Malcom, C., 1990, Glass from Nuestra Señora de Atocha, *Journal of the Mel Fisher Maritime Heritage Society*, **6**(**1**).

Marks, R., 2006, Stained glass in England during the Middle Ages, Routledge.

Marvasi, M., E. Vedovato, C. Balsamo, A. Macherelli, L. Dei, G. Mastromei, and B. Perito, 2009, Bacterial community analysis on the Mediaeval stained glass window “Natività” in the Florence Cathedral, *Journal of Cultural Heritage*, **10**(**1**), 124-133.

Mateo, M., G. Nicolas, V. Piñon, A. Ramil, and A. Yañez, 2005, Laser cleaning: an alternative method for removing oil-spill fuel residues, *Applied surface science*, **247**(**1-4**), 333-339.

Maurice Drake, F., 1928, The Technique of Stained Glass, *Archaeological Journal*, **85**(**1**), 80-90.

Melcher, M., R. Wiesinger, and M. Schreiner, 2010, Degradation of glass artifacts: application of modern surface analytical techniques, *Accounts of chemical research*, **43**(**6**), 916-926.

Merkel, R., S. Gruhn, J. Dittmann, C. Vielhauer, and A. Bräutigam, 2012, General fusion approaches for the age determination of latent fingerprint traces: results for 2D and 3D binary pixel feature fusion: Three-Dimensional Image Processing (3DIP) and Applications II, p. 82900Y.

Millis, D. L., and D. Levine, 2013, Canine rehabilitation and physical therapy: Philadelphia, Elsevier Health Sciences.

Murcia-Mascarós, S., P. Foglia, M. L. Santarelli, C. Roldán, R. Ibañez, A. Muñoz, and P. Muñoz, 2008, A new cleaning method for historic stained glass windows, *Journal of Cultural Heritage*, **9**, e73-e80.

Nimmrichter, J., W. Kautek, and M. Schreiner, Sept. 21–25, 2005, Lasers in the Conservation of Artworks; LACONA VI Proceedings: Vienna, Austria, Springer.

Piñar, G., M. Garcia-Valles, D. Gimeno-Torrente, J. L. Fernandez-Turiel, J. Ettenauer, and K. Sterflinger, 2013, Microscopic, chemical, and molecular-biological investigation of the decayed medieval stained window glasses of two Catalonian churches, *International biodeterioration & biodegradation*, **84**, 388-400.

Pouli, P., 2000, Laser cleaning studies on stonework and polychromed surfaces: Doctoral thesis, Loughborough University, Loughborough.

Pouli, P., D. C. Emmony, C. E. Madden, and I. Sutherland, 2001, Analysis of the laser-induced reduction mechanisms of medieval pigments, *Applied Surface Science*, **173**(**3-4**), 252-261.

Pradhan, S., K. A. Keller, J. L. Sperduto, and J. H. Slater, 2017, Fundamentals of Laser‐Based Hydrogel Degradation and Applications in Cell and Tissue Engineering, *Advanced healthcare materials*, **6**(**24**), 1700681.

Quintana, C. L. S., 2016, Development and optimisation of protocols for surface cleaning of cultural heritage metals: Master's thesis, University of Évora, Évora.

Römich, H., K. Dickmann, P. Mottner, J. Hildenhagen, and E. Müller, 2003, Laser cleaning of stained glass windows–Final results of a research project, *Journal of Cultural Heritage*, **4**, 112-117.

Römich, H., and A. Weinmann, 2000, Laser cleaning of stained glass windows. Overview on an interdisciplinary project, *Journal of Cultural Heritage*, **1**, S151-S154.

Raguin, V. C., 1988, Conservation and Restoration of Stained Glass: An Owner's Guide, Atlantic Books

Raguin, V. C., 2013, Stained Glass: Radiant Art, Getty Publications.

Rea, E. C., 2004, Scribing of thin sapphire substrates with a 266-nm Q-switched solid state laser: Photon Processing in Microelectronics and Photonics III, p. 231-241.

Riveiro, A., A. L. Maçon, J. del Val, R. Comesaña, and J. Pou, 2018, Laser surface texturing of polymers for biomedical applications, *Frontiers in Physics*, **6**, 16.

Rodriguez-Navarro, C., K. Elert, E. Sebastian, R. M. Esbert, C. M. Grossi, A. Rojo, F. J. Alonso, M. Montoto, and J. Ordaz, 2003, Laser cleaning of stone materials: an overview of current

research, *Studies in Conservation*, **48**(**sup1**), 65-82.

Romich, H., K. Dickmann, P. Mottner, J. Hildenhagen, and E. Muller, 2003, Laser cleaning of stained glass windows - Final results of a research project, *Journal Of Cultural Heritage*, **4**, 112S-117S.

Royce-Roll, D., 1994, The colors of Romanesque stained glass, *Journal of Glass Studies*, **36**, 71-80.

Rubahn, H.-G., 1999, Laser applications in surface science and technology: Chichester, John wiley & sons.

San Casciani, P., 1989, The technique of decorative stained glass, Courier Corporation.

Schabereiter-Gurtner, C., G. Pinar, W. Lubitz, and S. Rölleke, 2001, Analysis of fungal communities on historical church window glass by denaturing gradient gel electrophoresis and phylogenetic 18S rDNA sequence analysis, *Journal of Microbiological Methods*, **47**(**3**), 345-354.

Schalm, O., K. Janssens, and J. Caen, 2003, Characterization of the main causes of deterioration of grisaille paint layers in 19th century stained-glass windows by J.-B. Capronnier, *Spectrochimica Acta Part B: Atomic Spectroscopy*, **58**(**4**), 589-607.

Schalm, O., K. Janssens, H. Wouters, and D. Caluwé, 2007, Composition of 12–18th century window glass in Belgium: Non-figurative windows in secular buildings and stained-glass windows in religious buildings, *Spectrochimica Acta Part B: Atomic Spectroscopy*, **62**(**6-7**), 663-668.

Schalm, O., V. Van der Linden, P. Frederickx, S. Luyten, G. Van der Snickt, J. Caen, D. Schryvers, K. Janssens, E. Cornelis, and D. Van Dyck, 2009, Enamels in stained glass windows: Preparation, chemical composition, microstructure and causes of deterioration, *Spectrochimica Acta Part B: Atomic Spectroscopy*, **64**(**8**), 812-820.

Seewig, J., I. Raid, C. Wiehr, and B. A. George, 2013, Robust evaluation of intensity curves measured by confocal microscopies: Optical Measurement Systems for Industrial Inspection VIII, p. 87880T.

Semwogerere, D., and E. R. Weeks, 2005, Confocal microscopy: Encyclopedia of Biomaterials and Biomedical Engineering: New York, Taylor & Francis.

Siano, S., 2008, Principles of Laser Cleaning in Conservation, in *Handbook on the Use of Lasers in Conservation and Conservation Science*, M. Schreiner, M. Strlic, and R. Salimbeni, eds., COST G7, Brussels, Belgium.

Siano, S., and R. Salimbeni, 2001, The Gate of Paradise: physical optimization of the laser cleaning approach, *Studies in Conservation*, **46**(**4**), 269-281.

Sloan, J., 1991, Is stained glass protective glazing necessary?, *New York Landmarks Conservancy, Common Bond Spring*, **7**(**2**), 4-7.

Sterpenich, J., and G. Libourel, 2001, Using stained glass windows to understand the durability of toxic waste matrices, *Chemical Geology*, **174**(**1-3**), 181-193.

Strassl, M., V. Wieger, D. Brodoceanu, F. Beer, A. Moritz, and E. Wintner, 2008, Ultra-short pulse laser ablation of biological hard tissue and biocompatibles, *Journal of Laser Micro/Nanoengineering* **3**(**1**), 30-40.

Van der Snickt, G., S. Legrand, J. Caen, F. Vanmeert, M. Alfeld, and K. Janssens, 2016, Chemical imaging of stained-glass windows by means of macro X-ray fluorescence (MA-XRF) scanning, *Microchemical Journal*, **124**, 615-622.

Vilarigues, M., P. Redol, A. Machado, P. Rodrigues, L. Alves, and R. Da Silva, 2011, Corrosion of 15th and early 16th century stained glass from the monastery of Batalha studied with external ion beam, *Materials Characterization*, **62**(**2**), 211-217.

Vogel, N. A., and R. Achilles, 1993a, The Preservation and Repair of Historic Stained and Leaded Glass, v. 33, US Department of the Interior, National Park Service, Cultural Resources, Preservation Assistance.

Vogel, N. A., and R. Achilles, 1993b, Stained Glass in Houses of Worship, Inspired Partnerships.

Weaver, J. L., J. S. McCloy, J. V. Ryan, and A. A. Kruger, 2016, Ensuring longevity: Ancient glasses help predict durability of vitrified nuclear waste, *American Ceramic Society Bulletin*, **95**(**PNNL-SA-118907**).

Wigelsworth, J. R., 2006, Science and technology in medieval European life, Greenwood Publishing Group.

Wirth, R., 2009, Focused Ion Beam (FIB) combined with SEM and TEM: Advanced analytical tools for studies of chemical composition, microstructure and crystal structure in geomaterials on a nanometre scale, *Chemical Geology*, **261**(**3-4**), 217-229.

WoisetschlaÈger, G., M. Dutz, S. Paul, and M. Schreiner, 2000, Weathering phenomena on naturally weathered potash-lime-silica-glass with medieval composition studied by secondary electron microscopy and energy dispersive microanalysis, *Microchimica Acta*, **135**(**3-4**), 121-130.

Wong, K.-y., 2016, The hidden gem from earthly paradise: technical guidelines for the conservation and maintenance of the stained glass of St Andrew's Church, Hong Kong: Master's thesis, University of Hong Kong, Hong Kong.